SEVENTH FRAMEWORK PROGRAMME
Area 6.4.1.2. Cross-cutting research activities relevant to GEO
ENV.2008.4.1.2.1. Monitoring and observing oxygen depletion throughout the different Earth system components

Deliverable D 2.4
Report on oxygen dynamics in silled basins and its dependence on atmospheric, marine, and terrestrial boundary conditions, including land-use and nutrient loading; month 36

Editors: D. Aleynik, H. Stahl, M. Inall , SAMS
with all partners of WP2

Project acronym: *HYPOX*
Project full title: *In situ monitoring of oxygen depletion in hypoxic ecosystems of coastal and open seas, and land-locked water bodies*
Grant agreement no.: *226213*

Date of preparation: *19. April 2012*

Contents

Oxygen dynamics in basins with restricted exchange: A case study of a Scottish fjord (Loch Etive, North-West Scotland)

Abstract

The hydrophysical regime in semi-enclosed water bodies with strong tidal influence and topographically restricted exchange with the open ocean has been the focus of numerous research papers in past four decades. Loch Etive is a Scottish fjord located in North West Europe which is exposed to the North Atlantic with low anthropogenic pressures. Yet the fjord experience aperiodic hypoxia in its inner deep basin which has been suggested to be mainly driven by natural factors such as bottom topography, tides and freshwater input to the fjord. In this study we focus on the main physical drivers of these processes controlling the delivery of oxygen enriched water from outside the fjord to the inner deep basin during the period December 2009 to January 2012. The study confirmed that the unusually cold winter of 2009/2010 was the controlling factor for the overturning event that took place in January 2010, whereas the consecutive 2 overturning events during dry spring and summer (2010) was facilitated by reduced fresh water supply from a nearby hydro-electric power installation..

Introduction

Fjords are common features of the mountainous western shorelines in high and middle latitudes in both the northern and southern hemispheres, which are commonly described as narrow, long and deep water bodies surrounded by steep slopes and at least one, but often more sills. Detailed reviews of physical oceanography of fjords were given in Farmer and Freelander [1983], with recent updates in Inall and Gillibrand [2010]. Detailed paper review of turbulent mixing processes in fjords is gathered in Inall [2005]. Many aspects of vertical mixing processes in stratified fjords in presence of tidal forces and internal waves are described by A. Stigebrandt [1976, 1977, 1980, 1981, 1999 and 2001].

Following the concepts outlined in the above mentioned studies, the current report consists of *5* sections. In *Section 1,* topographic constraints of the studied fjord system is given. A brief description of the observed physical processes determining water dynamics in Loch Etive is presented in *Section 2.* In *Section 3* external forcings applied to the open boundaries of Loch Etive and its surface during the experimental period is characterized. In *Section 4* focuses on the description of a 3D numerical coastal ocean model, specifically designed for Loch Etive. Finally in *Section 5* certain modelling validation test results are compared with available observations, followed discussion and conclusions in *Section 6*.

Section 1

Topographic restriction of water exchange

Glacially overdeepened trough are a common features of NW European coastline, and one of them Loch Etive has been eroded by ice moving in SW direction down the loch in several sequential glaciations during the last 2 Ma [Howe et al, 2001]. The latest European ice coverage scrapped soft sedimentary material previously covered valley surface and its steep sides. In the upper basin the bottom slopes are 5-15° in the deepest part (>100 m), reducing to 2-5° in its shallower (<50 m) section.

In the fjord-narrows irregular hard bedrock (granite) outcrops has been exposed, and glacially scoured hollows for the latest sediments accumulation has been formed behind them. According to seismic sonar survey (boomer), confirmed by several gravity cores [Howe et al 2002], a 30-50 m thick sediment layer has accumulated in the upper part of the deep basin of Loch Etive since the last glacial re-advancing (Younger Dryas, 10ka BC), as a result of two stage deposition. Initially the deposition originated from glacio-marine input, which later shifted to a large riverine load, resulted in a very high sediment accumulation rate (0.5 cm per year) in the Loch, in conditions of relatively low energetics of near bottom currents. While in Scandinavia postglacial rebound is significant (up to 8 mm/year) [Paulson et al, 2007], the western Scottish postglacial land mass uplift is nearly in a balance with the slow sea level rise, which according to satellite altimetry globally is 2.9-3.4 mm/year [Nerem et al, 2010] and has local variations of few ±mm/year in North Atlantic if halosteric contribution is taken into account [Ivchenko et al, 2008].

Since the land ice melted the main external forces affecting water circulation in fjord are tides, wind, freshwater discharge, precipitation, and vertical structure of thermohaline fields in the nearby seas. Observed variations in the sediment flux (from sediment core data) are primarily attributed to natural oscillations (i.e Medieval Warm / Little Ice Age), while anthropogenic changes (deforestation) could have masked this signal [Nørgaard-Pedersen et al, 2006].

The bathymetry of Loch Etive is shown in **Fig. 1.** Shallow sills are combined with narrowing of the coastline not only at the very entrance to the fjord (220 m width at Falls of Lora, but also in the upper part of this six-sill basin (200 m at Bonawe). In **Tables 1** and **2** details about the sills and basin geometry are given based on Edwards, Sharples [1991]. Recent mean depth of the sills has been re-estimated with data from extensive multi-beam CUBE survey (J. Howe, pers. communications) and the values vary in average between 6 and 13 m, with maximum in a sill 5 which has depth 24 m. Length of the sills along the Loch range from 240 m to nearly a 2 km wide shallow plateau in Ardmucknish Bay. Overall average width of the loch is approximately 2 km. The Loch can be divided in to two main basins separated by the 13 m deep Bonawe sill; the lower basin with a maximum depth of 70 m and a surface area of 11.4 km^2 and the upper basin with a maximum depth of 145 m and surface area of 16.9 km^2. There is a right-side asymmetry with range of 5-15º in surrounding upper basin very steep slopes defined as a result of collision of two glacial streams along the trough axis.

Experiments with Weather Regional Forecast model (WRF2.3) revealed essential tunnelling effect from local orography. High hills and mountains are located on both sides of the fjord: Ben Cruachan 1126 m on the eastern side and Beinn Mheadhonach 750 m and Beinn Molurgainn 690 m forming steep slopes on the western side of Loch Etive. As a result the south-easterly winds blows down the loch, while south-westerly winds blows in a landward direction along the loch axis (Fig**. 2a,b**). Locally winds can be even more enhanced by narrow Glen's, like Glen Noe next to HYPOX mooring base station, which is known for accelerating the winds along the northern slopes of Ben Cruachan.

The geometric constrains around the Loch affect the water flow in a different ways. Geometric reduction in vertical cross-sectional area obviously leads to acceleration of fluid flow of according to Bernoulli's principle and law of energy conservation. Accelerated flow increases a friction against the sea bed in proportion to the square of the current speed, which, in turn, decreases the volume of water passing through the fjord entrance due to skin friction. In the widening areas behind the narrow sills of the Loch where flow is slowing down again, series of energetic eddies are produced due to barotropic form drag. The density stratification in the water column in the presence of sill will produce an additional form of frictional drag associated with the tidal oscillations. A critical value of the relation between degree of stratification and flow speed, which is referred as baroclinic form drag, can be calculated. All these processes will be considered in more detail in the next section.

Section 2

Physical Processes in Loch Etive

Stratification

Temporal variation and structure of the vertical density stratification in a sea loch is generally different from adjacent coastal parts of the sea, where the seasonal cycle of thermal stratification is a dominant feature. In a loch a combination of topographic restrictions and high volume of fresh-water input is able to shift a stratification dependency from thermal to salinity dominated, even without a clearly detected seasonality. The latter is a typical feature for the upper deep basin of Loch Etive, which can remain isolated for prolonged periods of time.

The only available previously annual cycle of full-depth observations, at 8 stations spread along the entire length of Loch Etive (REES experiment in 1999-2001, **Fig. 3**), revealed the presence of a seasonal signal in upper 30-40 m of water column. Seasonal variation for surface temperature is in a range of 4 – 16 ºC (**Fig. 3a**). At the sea surface, salinity varies from 22 to 1 psu (after heavy rains) (**Fig. 3b**). The salinity seasonality detected in upper 30-40 m of the water column is typically associated with increased fresh water runoff in the autumn/winter period. Dissolved oxygen concentrations in Loch Etive in the upper subsurface layers followed mainly a thermal seasonal signal and varied between 7 – 10 mg $O_2 \cdot l^{-1}$ (**Fig. 3c**). In the isolated upper basin layers below 40-50 m neither thermal nor salinity seasonal signals were detected during both the REES and HYPOX projects (2010-2011 time series shown on **Fig 4a,b**).

Fresh water supply

Loch Etive has the largest ratio between its watershed and sea surface area (45:1) of all Scottish sea lochs, which leads to large annual fresh water input, accumulated from 12 rivers. The major river discharging into Loch Etive is the Awe River, which has a catchment area of 828.6 km^2 and delivers 60-66% of all the fresh water into Loch. The fresh water input from the rest of the sources can be evaluated using the precipitation rate from nearby weather stations and its catchment area, which for upper basin is 154.8 km^2 (excluding r. Awe) and for the lower one is 277.8 km^2 (Table 2.3 in Magill et al, 2008, p. 16 – 17). The overall Loch Etive watershed is estimated as 1350 km^2 [Edwards and Sharples, 1985]. The range of total annual precipitation in the area, estimated to 2000 – 3000 $mm \cdot year^{-1}$, is accompanied with seasonal and inter-annual variations associated with dominating weather pattern over the North-East Atlantic.

The fresh water discharge rate from river Awe is controlled by the 25MW Inwerawe hydro-electric power station since 1963 (Miller, 2002). Loch Awe water supplies a single turbine via an underground tunnel from the Awe Barrage. Data for the fresh water discharge into the Loch Etive based on the detailed daily mean flow from river Awe, Barrage Gate and freshets for period 2009/12 – 2011/07, was provided by courtesy of Scottish and Southern Energy. Discharge rates for the other rivers was produced using multiplication of their catchment area, hourly rainfall rate (**Fig. 5a)** from Dunstaffnage Weather Station (DWS), and the season-dependant

evapo-transpiration factor (ET). The latter was estimated as a sinusoid with the highest value (0.9) in winter, and lowest in summer (0.7). Some uncertainties remain in these estimates associated to the different residence times of the precipitated waters in various soils,the porosity of the underlaying substrates, vegetation types (upper basin has more woodlands, while lower basin mainly provides livestock and sheep farming), exposure of mountain slopes to prevailing winds and a number of other parameters used in more precise and complex evapotranspiration models [Portilla, Tett, 2008; Young, 2006]. We can assume that these differences are minor in comparison to the main and manually (automated since maintenance in 2009) regulated riverine source (river Awe).

The combined data set for fresh water supply exhibits a high variability during the latest period of the observation (**Fig. 5i**). The lowest level of rainfall occurred between January – July 2010 which was estimated as 77% of the long term average (lta, 1971 – 2000).This corresponds to the lowest river flow (58% of lta) in the West Highland region of Scotland, according to the Centre for Ecology and Hydrology (CEH reports, 2010-2011). Notably the lowest river flow (29% lta) was measured in December 2009, the month prior to the first overturning in the Loch Etive during the period of HYPOX experiments. In stark contrast, 2011 was both the warmest (2^{nd} since 1910) and the wettest year on record, with an estimated annual rainfall of 138% lta and river flow125 % lta.

Heat fluxes

A thermally driven seasonal cycle in upper layers of Loch Etive, associated with seasonal variations in the heat flux, was clearly detected by the sub-surface instrument (Seaguard) deployed at the HYPOX observatory site at 14 m depth in the upper basin (**Fig. 1**). Red lines in **Figure 4** show variations in Temperature (a), Salinity (b), Potential density (c) and Oxygen (d). Similar and coherent seasonal variations with the depth-related lag were found in data from SAMS PSIT Sea-Bird SBE16 instrument in Airds bay (22 m depth, green line, **Fig. 4**). The moorings at Saulmore (9 m) near the loch entrance and at the Foram point (30 m) in adjacent part of the Firth of Lorn, was deployed by NERC Diving Unit research team.

Breaking of the stratification due to both an excessive heat loses associated with a net long wave radiation and sensible heat loses associated with the largest temperature differences between the sea surface and air is a rare scenario for a moderate climate of the western Scotland, but it was observed (at least once) in a nearby Clyde Sea in late autumn [Rippeth, Simpson, 1996].

In the bottom waters there was no seasonal cycle observed for the duration of whole HYPOX experiment (**Fig. 4**, magenta line for data from RDCP-600 instrument deployed at 124 m). Instead the observed parameters in the isolated deep waters of the upper basin are only slowly modified by a number of mixing- and biogeochemical processes taking place in the deep water.

Barotropic exchange and renewals

The other important source of changes for deep water stratification (renewals) are the processes of *barotropic exchange*, mainly associated with a) *tidal advection* of external (to the Loch) waters over the sill into the upper basin, which may lead to partial or whole displacement of deep waters within the Loch, b) storm surges and c) mean sea level rise.

Lateral and bottom friction cause the amplitude of the tide in Loch Etive to be smaller (2.3 m at Bonawe sill) inside than outside (4.1 m in Oban bay and Connel). Frictional resistance of the loch system to barotropic tidal flow result in asymmetric delay in time of arriving of slack (low speed) relative to the time of high and low waters. Phase lag between high waters at the loch entrance in Connel and the Bonawe sill is estimated to 1 hour and 50 minutes (Poltips-3 model).

At the narrow and shallow sills during a peak tide, currents are almost purely barotropic, and hence directed one way, while in transition between flood and ebb phase, two layer transports may also exists [Stigebrandt, 1977]. The maximal values for barotropic velocity in Connel narrows can be estimated using the data from Tables 1 and 2 for Loch Etive and the formula $u_b=T^{-1}aY/BH$ [Stigebrandt 1977] where tidal amplitude a=4.1 m, tidal period $T=4.5\cdot10^4$s, loch area $Y=29.5\cdot10^6$ m^2, sill width B=320 m and sill depth H=6 – 13 m, g=9.81 $m\cdot s^{-2}$, density of waters inside and outside the loch are $\rho_1\approx\rho_2\sim10^3$ kg m^{-3}, $\Delta\rho$=2 kg m^{-3}. If all required conditions, such as the interface between layers ρ_1 and ρ_2 is lower than sill depth, transition between loch and open sea is short (few km) or similar to the excursion length of fluctuating currents, are satisfied, then $u_b=2\div4$ m s^{-1}. The highest reported surface velocity from the entrance sill at the Falls of Lora is 8 knots during ebb spring tide [Wilding et al, 2005], while at the upper Bonawe sill it is 2.5 knots (according to Admiralty charts).

Two other processes related to sea level rise can increase pressure gradients along the loch, and consequently increase the transport across the sill. The mean sea level in upper Loch Etive is a little higher than at its entrance due to the total volume of fresh water input. The inverse barometer effect could produce additional sea level rise in sea lochs. All three observed renewals events in 2010 match in time with a fall in atmospheric pressure (**Fig. 7,8,9 g**) and rough estimates for storm surges (10 mm per 1 hPa) produce a rise of about 0.3 m, which is 8 (13) % of the maximal spring (neap) tidal range. Geometric restrictions and tidal velocities at the fjord entrance are the main regulators for the transport capacity of the sill, and therefore define the quantity of dense saline waters delivered to the upper part of the basin [Stigebrandt, 1977, 1980].

Baroclinic exchange

Fluctuations in riverine input and meteorological parameters at the sea surface give rise to differences in the density stratification along the loch itself and between the loch and the adjacent sea (Firth of Lorn). This density difference generates pressure gradients which impose the driver for baroclinic flow, even in the absence of friction.

Some parts of Loch Etive with deeper sills on the seaward entrance, like in Airds bay, can be defined as a highly stratified estuary [Wood et al., 1973]. The ratio between the volume of fresh water input *R* and the volume of sea water *V* delivered to this fjord during a tidal cycle is close to one or higher, and hence the mixing across the interface separating the fresh waters from the deeper saline waters is weak, and therefore, the compensational *estuarine circulation* is weak as well. In case of weak tidal forcing, intermediate circulation in layers between the thin surface brackish layer and the intermediate water layers above the sill depth is driven by internal vertical oscillations in the pycnocline outside the fjord. In Norwegian and Swedish fjords the intermediate circulation are commonly related to wind driven coastal upwelling [Arneborg, 2004].

Another sequence of water stratification in the presence of strong barotropic flow acceleration over the sill is the process of *aspiration* of more dense waters from the depth below the sill upwards and across the sill. This process is driven by the pressure gradient which is depth irrelevant. On internal side of the sill this aspirated water tends to sink toward its equilibrium depth, which is expected to be higher than the initial depth due to the reduction in the density by mixing with the inner loch waters on a way over the sill. Partial or entire displacement of intermediate and deep water inside the loch by this type of intrusions is defined as *overturning* or *renewal* events (EE77). The timescale of renewal events depends on the rate of downward buoyancy flux, which is determined by vertical, and to a lesser degree, horizontal mixing of more fresh sub-surface waters with interior waters. The two renewals events observed in Loch Etive in 2010 happened on duration of several tidal cycles (2 – 3 cycles in February and 10 cycles in June).

*Wind*s affect both vertical mixing and horizontal transport in relatively shallow and stratified lochs. In case the sides of the loch valley are high the winds in general steer along its axis. Up-loch winds push the shallow fresh water farther up the loch, generating a compensational flow downward. While for winds blowing the opposite way, i.e. down the loch, enhanced estuarine circulation could contribute to renewals, as observed by [Gillibrand, et al 1995] in Loch Sunart. Rapid reduction of wind stress can cause fast flattening of isopycnal surfaces which results in long lasting seiche oscillations, especially if the basin size matches with half of the internal wavelength [Cushman-Roisine et al, 1989]. Wind induced vertical mixing can be even higher than tidally induced mixing as shown in fjords on the west coast of Sweden [Arneborg, Liljebladh, 2001].

Earth rotation can affect water motion by creating right asymmetry (in northern hemisphere) if the width of the basin is higher or equal to the baroclinic Rossby radius *R*, which is proportional to the phase speed of internal waves and thus to the square root of stratification. At Scottish latitudes *R* is a few km. Even if this effect is minor in high latitude fjords, in the wider basins of Loch Etive such as Ardmucknish- and Airds bay, this steering and increasing of baroclinic inflow currents along the right shore and outflow currents along the left shore due to Earth's rotation are not negligible.

Vertical exchange and mixing

Turbulent mixing in fjords is a part of a major global irreversible process which tends to homogenise formerly stratified waters by uplifting denser water and moving lighter waters downward, thus increasing the potential energy (PE) of the water column. The main source of energy required to complete the mixing is the turbulent kinetic energy (TKE), which is derived from either instability of the mean flow or by convective instability due to sea surface cooling/heating. The latter is relatively rare event in high latitude fjords, especially in a presence of strong salinity stratification. To estimate mixing efficiency the relation between portions of TKE released to increase the potential energy and that lost in dissipation is often used. The three main mechanisms of energy loss from tidal flow in geometrically restricted conditions defined by Stigebrandt (1999) are: 1) momentum of mean flow lost in turbulent dissipation in a bottom boundary layer due to friction against the seabed; 2) tidal flow that emit shedding eddies and even separates from bottom boundary because of increasing cross-sectional area behind the sill (barotropic form drag), and finally 3) internal baroclinic waves, generated by oscillation in pycnocline, at frequencies close to tidal, propagates free toward the fjord head and toward the sill and extracts the energy from barotropic flow.

Suggestions about the energy loss due to horizontal eddy shedding and internal wave radiation are consistent with the observations from Knight Inlet (Farmer, Armi, 1999) and from Loch Etive (Inall, et al 2004), where fortnightly variation of external barotropic tides resulted in periodic regime changes from a '*tidal jet'* during spring tides with flow separation from the bottom at ~35 m (3 times of sill depths) on its lee-side, to a '*wave regime*' during neap phase, when mode-1 baroclinic wave response become dominate feature. Direct measurements of the flow over the sill gave the estimates of relative weight for these components of energy dissipation processes: due to bottom friction, barotropic form drag and freely radiating baroclinic waves drag in a ratio 1:4:1 (1:4:3.3) at springs(neaps), according to (Inall et al 2004). In that paper, the estimation for lee-wave drag is assumed to be an order of unity, similar to (Baines, 1995). Contribution from breaking of internal waves in the basin interior is estimated to 0.2. Less effective for mixing is the process of internal waves of breaking in the approach of the sea loch sloping boundary as revealed in a recent dye-release experiment (Inall, 2009). A more efficient process was observed in the area next to the Bonawe sill during the flood phase, when vertical mixing is intensified as an internal hydraulic jump occurs (Inall, 2005). The mixing can be even more enhanced by the arrival of internal waves, reflected from the basin head and slopes.

Non-linear wave generation, energy dissipation processes and particularly bottom friction effects and lee-wave drag in basins with sill geometry similar to the upper part of Loch Etive were the focus of a detailed study carried out using 2-D slicing of high resolution non-hydrostatic models [Stashchuk et al, 2007; Xing, Davies, 2009]. In the highly varying environments the frequency of deep basin overturning events directly dependent on the efficiency of a vertical mixing below sill depth and potentially can be determined with full 3D modelling approach with precisely defined initial and open boundary conditions.

Isolation of deep waters and oxygen depletion

Facing the facts of accelerating climate change, especially pronounced in polar regions, it is likely that it will have an effects on the oxygen conditions in Loch Etive. Increasing surface temperatures and precipitation rates will potentially enhance water column stratification and restrict exchange of deep isolated water bodies even further. Additional input of terrestrial organic matter due to an increased river runoff as well as higher temperatures will most likely increase the biological oxygen demand as well as the solubility of oxygen. Thus, expected climate change may significantly increase the severity of hypoxia in Loch Etive, a fjord that already is classed as one of the most sensitive lochs in Scotland in terms of oxygen depletion [Gilibrand et al 2007].

In the absence of renewal events the isolated deep waters of fjords and sea lochs tend become stagnant, nutrient enriched and depleted in oxygen [Stigebrandt, Aure, 1989; Gillibrand et al, 1996]. This is mainly due to the bacterial and faunal degradation of accumulated organic matter, a process that consumes available dissolved oxygen while releasing nutrients and carbon dioxide into the water. Hence, the degradation of organic matter tends to increase the Biochemical Oxygen Demand (BOD) and reduce the oxygen concentration in the bottom water and in surficial sediments layers, which can reach hypoxic levels (>2mg O_2 L^{-1}), with subsequent negative effects on both the benthos and pelagic ecosystems. The probability of the hypoxia in a deep basin is determined by two timescales: 1) time span between successive renewals and 2) the time it takes to consume the available oxygen in the isolated deep water. Factors affecting these time scales, according to Gillibrand et al [1996] are: a) the mixing rate of deep water, supplying deeper layers with oxygen rich waters; b) changes in average basin density required to overturning event to happened; c) oxygen consumption rate, which depend on POM supply; d) and the initial concentration of oxygen in newly formed deep water .

Particulate organic matter input to Loch Etive is dominated by allochtonous supply (Overnell et al. 1996; Loh et al 2002) although 30-40% of the POC in the sediment could be of marine origin (Malcolm & Price, 1984). Gross annual primary production in Loch Etive has been estimated to 70 g C m^{-2} yr^{-1}(Wood et al 1973). The primary production is not nutrient limited but light limited according to McKee et al. (2002). The organic carbon content of the sediment is high due to the high sediment accumulation rates of POC (0.50-0.87 cm yr^{-1}). The former contributes to the benthic oxygen demand, and average oxygen fluxes between 7.9 – 22.8 mmol O_2 m^{-2} d^{-1} has been recorded in the deep basin (M. Harvey, unpublished results) and 9.8 – 15.1 mmol O_2 m^{-2} d^{-1} in Airds Bay. These oxygen fluxes are mainly driven by bacterial and faunal respiration in the sediment, although abiotic reactions such as reoxidation of reduced compounds (e.g. Mn^{2+} and Fe^{2+}) have been shown to play an important role in Loch Etive (Overnell et al. 2002).

Aquaculture is a common feature in Scottish Sealoch's that can lead to organic matter enrichment and increased biological oxygen demand underneath and around the farms. In Loch Etive aquaculture is sparse and mainly dominated by mussel farming in the upper basin. In the past three decades Loch Etive have produced up to 1/3 of all Scottish farmed mussels, a 1000 tonnes in the peak year of 2000 [Magill, 2008]. However, the level of particulate organic matter (POM) related to aquaculture in Loch Etive has been reduced significantly in recent years, while the natural sources remain the same.

Deep water renewals in Loch Etive

Vertical distribution of dissolved oxygen along the Loch Etive axis according to 8 CTD casts undertaken soon after winter 2010 renewal events, one year (spring 2011) and two year (spring 2012) later are shown on **Fig 3.2.** Values of oxygen concentration in the deep part of inner basin reduced from 9 to 2 mg L^{-1}.

Reducing the difference between surface density at the sill and the water density in the deep basin could potentially lead to an overturning event, which means replacing the deep stagnant waters of the upper basin with denser Firth of Lorn waters from the lower part of the loch. The latter has direct connection to the open ocean over the Falls of Lora sill at Connel. The most important external factors which potentially can trigger the start of an overturning event in narrow fjords with multiple sills include: a) essential reduction in runoff in preceding week(s) [Edwards, Edelsten, 1976, 1977]; b) preferable down-fjord wind [Bell, 1973] which can enhance the compensation inflow current; c) similarly increasing of fresh water input in a basin could increase density (salinity) of the compensation underflow [Gilmartin, 1962]; d) lateral movements of waters in adjacent part of the ocean, delivering denser waters toward the coast and fjord sill [Saelen, 1947], associated with alterations in ocean scale wind driven circulation [(Dickson, 1973] or coastal upwelling [Anderson, Devol, 1973; Arneborg, 2004]. Since the work of Edwards and Edelsten (1977, from here EE77) the changes in fresh water runoff were considered as the main factor for Loch Etive renewals. Verification of the influence of other possible factors on the recent renewal events in Loch Etive is the focus of the present study.

Section 3

External forcing in 2010-2011

Recent monitoring activity

Two recently deployed AANDERAA instruments, on a cabled observatory mooring, produced 2 year-long time series (Dec 2009 – Dec 2012) for near-surface (Seaguard RCM-11 at 14 m depth) and near-bottom (RDCP-600, 124 m) layers in the deep upper basin of the Loch Etive. The location of the HYPOX cabled observatory and all the other mooring sites is shown over bathymetry on a map on **Figure 1**. In the lower part of the loch a 11-month long deployment with a standalone Seabird SBE-16 CTD (Airds Bay, 23 m) was done (Nov 2009 – Oct 2010) . Two other sites, maintained by the NERC Diving Unit, with temperature loggers were on a survey close the entrance to basin at Sualmore point at depth 10 m, and at the Foram point at 30 m with an option to recover data in delayed mode once-twice a year. Since December 2011 another mooring with a 4.5-m long thermistor chain (Access #11) was deployed close to the entrance of the loch, which transmits the vertical temperature profile from sub-surface layer in a real time (every 3 hour) using Iridium satellite communication. Additional information was available from irregular individual CTD casts throughout the year and several bio-geochemical and geophysical experiments randomly distributed in time and location.

Combined data, obtained between December 2009 – January 2012 from HYPOX and Airds bay moorings are shown on **Figure 4**. As expected for moderate latitudes it is the seasonal cycle that is the dominating feature for both Temperature and Salinity records from all surface and sub-surface instruments (**Fig. 4a-b**). While in the deeper part of Loch Etive the observed situation was the opposite. There were no signs of presence of seasonal cycles, but three abrupt changes in temperature and salinity values (HYPOX mooring, depth 124 m). The most dramatic change in water properties happened between 7 and 17 January when the bottom water overturned in the deep upper basin. A smaller overturning event also took place in February 2010 and finally significant overturning event was again observed in the end of June during year 2010 (**Fig 4a-b**). All three overturning events took place within the first 7 months during 2010, something that has never been recorded before. The bottom waters of the upper basin has stayed isolated since then, and no overturning event has been observed for more than **21 months**. According to (EE77) the time gaps between 11 sequential overturning events in Loch Etive from historical data could vary from few weeks to 2.5 years, with their model-estimated an average value 16 month. The magnitude for each of the three overturning events in 2010 was different in all cases.

The severely cold and dry winter of 2009/2010 and the unusuallydry spring and summer of 2010, followed by the warm but windy winter of 2011/12 exhibit the entire range of natural weather conditions in the area of Loch Etive, which potentially can be considered as the triggers for the overturning events of 2010 and the following isolation of the deep waters in the upper basin.

The first overturning in January 2010

In figure **7** we present available meteorological information and temperature records zoomed in to the period of January 2010. The dashed blue line at (**Fig.7, II**) represents the temperature value from the deep instrument (RDCP600, 124 m) at HYPOX mooring site, which drops from from 12.01 ºC to 7.73 ºC between Dec 2009 and Feb 2010. The observatory collected no data between end of December 2009 to beginning of February 2010 due to a power cut at the landward base station. Hence, the exact moment of the renewal event was not measured directly at this time. However, the assumption that newly replaced deep water should have the same temperature as the surface waters at the sill in the certain moment in time between Dec 2009 and Feb 2010, give us the time span for renewal event. This took place on 06-17 January 2010, as can be seen from the data of the temperature loggers, deployed at depth 9 m near the loch entrance at Saulmore point (red line), crossed by blue dashed line and extrapolated backward in time form actual measurements on the 4th February (Fig.**7, II)**.

Meteorological data zoomed in to the period of the first renewal event also coincided in time with a period of very low fresh-water supply (Fig.**7 *III*)**. Both water discharges at the Awe Barrage and at the Inverawe Power Station was truncated to the minimum level, required by regulations. Furthermore, there were very little amount of precipitation during 2-3 weeks before the event. The period of negative night air temperatures in December 2009 and January 2010 was extremely long for the area. Both these factors lead to storage of precipitated waters in a form of snow and ice, which additionally reduced stratification in upper basin. The first significant rainfall in the new year of 2010 took place on the 15th January (Fig**.7, *Ia***), which was followed by enhanced discharge from the rivers into Loch Etive (Fig.**7, *III***). Weekly average values for total amount of fresh water released in the first two weeks in January was only about $6 \cdot 10^6$ m^3, which dramatically increased (~10 times) during week 3.

Wind direction in the first half of January at Dunstaffnage was mostly from the east and southeast, and turned to south-west again during 17th January 2010 (Fig**. 6**). Taking topographic wind steering into account, we assume that the wind direction and speed at Dunstaffnage weather station (wind rose shown at Figure 6) correlates well with the winds near the sill. In a period between 6-16 January 2010 the wind was mainly sea-ward, which potentially leads to increasing of compensation flow of heavier and saltier water from the Firth of Lorn toward the sill area. Obviously, the overturning was only possible during the flood phase of the tide, when heavier and colder waters were able to pass the sill toward the fjord head with strong (up to 2.5 kn) currents. The smallest tidal amplitude in the area was on 10th January (neap), while the highest (spring) were on the 3rd and 17th of January. Replacement of the stagnant waters in the upper deep basin most likely lasted for one week (EE77), and finished whist the stratification in the upper layer associated with increased fresh water input after 15th January 2010, re-established. Particular details of the first overturning event and its duration and dynamics remain unclear due to the failure of the power supply to HYPOX cabled mooring and lack of data for this period. However, two other overturning events in 2010 were recorded in full detail (see below).

The second overturning 16-17 February 2010

The second overturning event of the deep waters in the upper basin, which took place between 16 and 17 February 2010, was recorded by the RDCP at 124 m depth. Meteo-parameters (***I. a-h***), temperature signals from both the upper (14 m) and lower (124 m) instruments (***II***) and river discharge data and estimates (***III***) for this period are shown on **Figure 8**. In comparison to the first overturning event, the drop in temperature in the near-bottom layer was less significant 1.1°C, from 7.73 to 6.64 °C. The change in salinity (0.1 psu), potential density (0.1 $kg \cdot m^3$) and in dissolved oxygen (from 300 to 335 μM) was also relatively modest. Series of small oscillations in temperature and salinity with amplitudes 0.3°C and 0.2 psu were observed during 3 weeks after the event. Salinity fluctuations at 124 m depth were coherent with the surface fluctuations (14 m) until it was damped and stratification was restored, which kept salinity unchanged for next 3.5 months. During most of February 2010, the river Awe discharge rate was below 20 $m^3 \cdot s^{-1}$ (Fig. **8, *III)***. Several days before the event, and soon after, there were negative night air temperatures, which bound an essential (but unknown) part of the precipitation (rain fall on 15th February) as snow and ice, hence temporarily reducing the freshwater supply from River Awe into Loch Etive, and the estimated discharge rates from the other rivers (Etive, Kinglass) was reduced accordingly.

The second overturning even coincided in time with the maximum spring tidal cycle (16 February 2010) and with large variations in the recorded temperature from the sub-surface instrument. The amplitude of the temperature oscillations, which lasted for a week, was up to 2.1 °C within a single tidal cycle. Simultaneously variations in the oxygen concentration in the upper and bottom layers went up in a range of 335 to 240 μM (88 – 65% saturation), and the latest one was substantially lower than the lowest measurements from Optode, deployed at 124 m (300 μM). This is the evidence of essential horizontal mixing process with entrainment of waters from the farther deep (not yet mixed) part of the basin.

Factors driving the second overturning could be summarised as the following: high spring tide, cold and salt waters approached the Aird Bay next to Bonawe sill, low fresh water supply in preceding weeks reduced stratification in upper basin.

The third overturning 22-28 June 2010

The onset of the last overturning, which took place 22-28 June 2010, began with very calm anticyclone weather conditions (1024 hPa, light easterly-north-easterly winds, 5-6 m/s, **Fig. *9, I)*** during the flood phase of the neap tidal cycle . The salinity stratification between the surface and bottom layers (27.5 psu) in the upper basin of Loch Etive was broken down during this week. As a result of the unusually dry winter, spring and early summer, low riverine input to Airds Bay allowed a pool of highly saline waters (29.7 psu) from Firth of Lorn to reach the upper basin and overturn the bottom waters due to its higher density. The the bottom layer temperature increased by 5 degrees (6.7 to 11.7 °C, Fig. ***9, II***) after the overturning, but the highly saline water was still dense enough to replace the bottom water in the inner basin. After the first precipitation in the

wet July (2010), salinity stratification was restored. That has resulted in more than 20 months (March 2012) of isolation, so far, of the deep bottom waters in the upper basin in Loch Etive, and the oxygen concentration is now close to hypoxia (i.e. 2 mg O_2 L^{-1})

The linear estimates for the mixing rates during observed stagnant period (522 days) since the latest renewal event in June 2010, was for temperature $3.9 \cdot 10^{-8}$ $^oC \cdot s^{-1}$, for salinity $5.7 \cdot 10^{-9}$ $psu \cdot s^{-1}$ and $5.2 \cdot 10^{-6}$ $\mu M \cdot s^{-1}$ for oxygen. The daily rates are $3.4 \cdot 10^{-3}$ $^oC \cdot s^{-1}$, $4.9 \cdot 10^{-3}$ $psu \cdot d^{-1}$ and 0.45 $\mu M \cdot d^{-1}$. Using Fick's law the estimates for vertical diffusion coefficients in the stagnant layers from the CTD casts taken in a deep basin on 26 August 2010 (day 57 after overturning) and on the 13 January 2012 (day 522) are shown in a **Table 3,** (the units are $m^2 \cdot s^{-1}$).

The currents velocity data from Aanderaa Seaguard instrument, deployed at 14 m depth, is available for two of the observed overturning events. The estimate of daily average residual current velocity along the loch axis (47.1°) at deployment site is shown at **Fig. 11**. During both overturning events in February-March and in June 2010 in sub-surface layer the 3-daily residual current (squares) was negative (outflow) in range of 4-6 cm s^{-1}. This is consistent with the hypothesis about the influence of strong down-fjord wind in that period in the inner basin.

Section 4

Numerical 3D model investigation of hydrodynamic regimes in loch Etive

Simplified approach to the problem of defining the frequency of overturning was successfully applied for several Scottish sea lochs with 3-layer box model ACExR (Gillibrand et al, 2012), which is an extension of FjordEnv model (Stigebrandt, 2001) for macrotidal fjord, programmed in the Matlab language. For the Loch Etive spring 2000 overturning event simulation the authors used daily average meteo-fluxes and boundary data (CTD profiles) obtained in Airds Bay (station RE6 next to the Bonawe sill), while omitting the other 5 sills. The basic details of average water mass parameters were captured well, with rms differences between model and observations of around 1 ºC and 1 psu. Effects of baroclinicity and nonlinear dynamics in a box model are traditionally parameterised with a number of tuning parameters and empirical coefficients, the best values for which are obtained with large series of ensemble runs.

Tidally driven circulation generates two distinct regimes in Loch Etive. One is the infrequent and intensive overturning which lasts only few hours/days. The inner basin deep water properties rapidly change by intensified mixing, induced by pulses of dense gravity current fluid intrusion along the inner sill slope.

The other process is a long lasting (month/years) transformation of stagnant isolated deep waters in the inner basin by slow turbulent mixing. Nonlinear processes associated with barotropic flow over the sill and internal tide generation on its lee side were in a focus of several local observations and experiments (Inall et al, 2004, 2005) and also in 2D-slice numerical non-hydrostatic models applied to Bonawe sill geometry (Xing, Davies, 2008; Stachuck 2007). Away from the sill the effects of hydraulic processes continue to have effect, but the scales are weak and occur generally above the interface which separates the stagnant deep layer from subsurface layer.

Simulation of the more realistic three-dimensional velocity, temperature, and salinity fields that are required by the companion bio-geo-chemical models was is the focus of the modelling studies now presented.

The first model implemented was the Proudman Oceanographic Laboratory Coastal Ocean Model (hereafter referred to as POLCOMS; Holt et al, 2001) adapted for Loch Etive. This model has been widely used in shelf and coastal studies around UK because of its efficiency and accuracy at a certain horizontal scale range. However, for structured-grid models the representation of realistic geometry especially around complex coastlines is a common difficulty, and hence reproduction of the currents there is generally poor. Insufficient volume transport in the narrow channels (3-4 grid cells with 50x50m horizontal grid resolution in the POLCOMS version implemented for Loch Etive) led to inability to maintain a realistic salt balance in the upper basin of the loch. This was a main reason for moving to the Finite Volume Coastal Ocean

Model (hereafter referred to as FVCOM; Chen *et al*., 2003) which has more geometrical flexibility. Usually finite volume models necessitate a relatively longer computational time compared with finite difference models, due to reduction in a time step required by Courant-Friedrichs-Levy (CFL) condition according to enhance horizontal resolution in certain areas. An effective parallelisation scheme developed for FVCOM (Cowles, 2008) allows running of the model on both small clusters and high-end computing resources (such as the HECToR supercomputer) with wide range of available processors. For example a one month long run required 10 hours of computer time on 192 processors.

FVCOM discretizes the integral form of governing hydrodynamic equations for transport and diffusion by solving numerically the fluxes across the boundary faces of non-overlapping prisms. In a horizontal plane the mesh consists of triangular cells, arbitrarily varying in size. The finite volume method of solving the system of primitive Navier Stokes equations has both advantages in computational simplicity of coding discrete structures similar to finite –difference methods and the geometric flexibility of finite-element scheme for irregular and complex coastlines. This method also ensures the mass–conservation in each single control element and in the whole computational area.

The model can be directly prescribed with a wide range of forcing data combinations, including tides, surface meteo-fluxes from weather station or output from meteo-models, river discharge and open boundary inflows/outflows. The latest version of FVCOM (3.1) was kindly provided to British unstructured models community by C.Chen with the help of R. Torres. We use built-in modules with the Smagorinsky scheme for horizontal mixing (Smagorinsky, 1963) and for vertical mixing we use the Mellor-Yamada level 2.5 turbulent closure (Mellor and Yamada, 1982). FVCOM was coupled with several nutrient, phyto- and zoo-plankton and bio-geochemical, sediment transport and ice modules (not used here). A brief description of the basic equations and the structure of these modules can be found in Chen et al. (2006). The number of successful FVCOM applications for simulating hydrodynamics and transport in lakes, estuaries and several more complicate mid-latitude and arctic fjords/inlet systems has increased recently (Forman, et al 2009; Chen et al, 2009), and more complete list of publications is available from the originators web site (http://fvcom.smast.umassd.edu).

The time period for our FVCOM simulation was chosen to be between January and July 2010, in order to overlap with the HYPOX physical sampling program and allow the most accurate evaluation of circulation patterns in the area during field activities. Although many scientific and technical issues arose with the model development and evaluation, we will be focus here on a subset of them, including (a) bathymetry smoothing and its effects on general circulation, (b) wind forcing and its influence on sub-surface circulation, (c) general model performance, and suggestions for improvements (including improvements in open-boundary time series, wind-direction and more accurate estimation of run-off).

4.1. Model setup and forcing: geometry

FVCOM adopts unstructured triangular mesh, and we used the recommended SMS10.1 software to build it. The mesh for the Loch Etive domain consists of 6601 elements (triangles) for velocity (u,v) and 3776 nodes for scalars (temperature, salinity, density, tracers). The horizontal scale of the mesh varies from 650 m at open boundary to 23 m in the main narrows at the Falls of Lora and Bonawe sills and at the river Awe inflow. For long term runs we used 15 unequally distributed terrain-following sigma-layers in the vertical, condensed in the upper and near bottom layers with an effective thickness varying from 0.15 m in the shallowest part of the domain to 18 m in deep basin respectively. For the short term process (overturning) simulation we increased the vertical resolution to 31 layers with an effective thickness range varying from 0.08 to 9 m. The trials with coarse resolution model demonstrate generally similar large scale features, but important small scale features were better represented by fine resolution model.

Model bathymetry was generated from the combined data set provided by S. Gontarek (SAMS), based on Admiralty charts and a side scan survey undertaken by SAMS in 1999-2000 in deep basin of the loch Etive (Howe et al, 2001). These data was updated with the results from a basin scale multibeam survey in February 2011 (J. Howe). The depth ranged from 0 m at shallowest coast to 145 m in deep inner basin. In Loch Etive regions shallower than 5 m occupies about 6 % of basin area and less than 2% of its volume. For such a steep sided shoreline and V-shape cross-sectional bathymetry, especially in the inner basin, the influence of a small flat intertidal zone on the overall circulation dynamics is insignificant. Therefore specifying the minimum model depth to a value close to the tidal range is a reasonable procedure, and for computational efficiency the capability for wetting and drying was not used

To avoid the problem of hydrostatic inconsistency found with sigma-coordinate ocean models (Haney, 1991; Mellor et al, 1994), we used bathymetric smoothing which set restrictions on the slope ratio $r_h=\Delta h/\Delta L$ between maximal depth difference Δh and the horizontal side length (ΔL) within each mesh triangle. The bathymetry smoothing thus applied had the additional restriction on preserving the overall basin volume and the volume of each individual triangular prism, similar to Forman et al, (2006 and 2009). The tests with different values of ratio r_h >1 demonstrates the appearance of spurious currents, excessive vertical mixing and abrupt fluctuation in temperature and salinity fields far beyond the expected range from available historical and recent CTD data (Fig. 2). Recommendations from (Chen et al, 2006) to use $r_h \leq$ 0.1 are unachievable without destroying regional bathymetry with narrow side walls, but reasonably stable T and S values (within the range of long-term observations) were obtained by setting r_h = [0.3–0.8] at the cost of compromised model depth at 7% of the nodes, located mostly next to the coast line. Extensive testing is still required in a search of the best fit between long model simulations and CTD profiles/time series and the fundamental model parameters.

4.2. Parameterisation and numerical considerations

For discrete volume flux integration FVCOM utilises a traditional time splitting of internal and external modes, as used in various oceanic models. CFL numerical stability conditions for an external (barotropic) mode can be determined as the ratio between horizontal scale (the side of the smallest triangle, *L*) and the sum of local velocity U and the phase speed of gravity waves, defined with acceleration due to gravity *g* and depth *H*:

$$\Delta T_E \leq \frac{\mathrm{L}}{\mathrm{U}+(gH)^{0.5}} \tag{1}$$

For the fine model geometry the upper bound of the shortest external time step was defined as ΔT_E=0.17 s. We reduced that value to 0.1 s to allow for the propagation of surface waves associated to sporadic strong tunnelling winds and the seiches, which are the fastest of possible modes. The internal mode time step defined as $\Delta T_I = I_{split}\ \Delta T_E$ and $I_{split}=10$.

For horizontal turbulence closure with the Smagorinsky eddy parameterisation we used a coefficient of C=0.1. Experiments with C=0.2 shows that flow regime become essentially more viscose and horizontal exchange slow down.

Vertical turbulence closure in this study was based on Mellor-Yamada 2.5 level model to resolve vertical eddy diffusivity K_m and vertical thermal diffusion K_h (Mellor and Yamada, 1982). We assign molecular kinetic diffusion $v=10^{-6}$ as the background value.

Bottom drag coefficient C_d in the model is defined with logarithmic-law by formula:

$$C_d = \max \left(\varkappa^2 \ \ln \frac{z}{z_o}^{\ 2}, \right. \\ C_{d0} \tag{2}$$

Where κ=0.4 is von Karman constant, Z_0 is the bottom roughness parameter and Z is the vertical distance from bottom to the nearest velocity grid point. Measurements of the very near bottom currents in the inner basin of Loch Etive are not available, but bottom visual data (photo and video) from the sill area and near shore rocks shows the presence of very strong near-bottom current able to move stones with settled seaweeds, while in the inner basin mud surfaces are nearly undisturbed, which confirm huge variability in the values of bottom roughness parameters along the loch. Since special variation of these parameters are not directly determined, we chose globally assign the minimal constant values C_{d0}=0.0025 and Z_0 *=0.003*, similar to those used by Forman et al (2009).

During the observation period the waters in loch Etive had been highly stratified in upper 10-30 m, with buoyancy frequencies N=0.1-0.2 s^{-1} (60–115 cph) and a weakly stratified layer below that depth with $N \leq 0.2 \cdot 10^{-2}$ s^{-1} (1 cph) Possible improvement of the MY2.5 vertical diffusion coefficient with an additional stratification- dependent term, which represents mixing

caused by breaking internal waves (Gillibrand and Amundrund, 2007) potentially, can increase basin scale vertical mixing. The tests with MY2.5 version however, demonstrate presence of excessive vertical mixing, which required to be suppressed, rather than exaggerated.

4.3 Tidal forcing

To force the model we used six main tidal constituents, listed in **Table 4.** These diurnal and semidiurnal constituents accounted for 79% of tidal height variance in Oban bay and were calculated from a long term sea level measurements at Northern Lights pier located on a distance 1.5 (4.1) miles from the nearest (farthermost) model open boundary points. We specified tidal elevations and phase along 16 open sea nodes and zero flow normal to the coast.

4.4 Fresh water supply

A key parameter to verify model performance is the ability to reproduce salinity (and temperature) variations within the model domain. To achieve this task we estimated daily fresh water discharge for the main 5 rivers (Awe, Etive, Kinglass, Nant and Noe), shown on Fig. 5(i) and panel III, Figs.7-9. To construction these time series we used the water shed values (Magill et al, 2008; Edwards and Sharples, 1985), seasonally varying evapo-transpiration factor (0.7-0.9) and daily estimates of precipitation rate converted from hourly data from the Dunstaffnage Met-Office station (Fig.5a), combined with daily measurements provided by Scottish and Southern Energy for river Awe barrage and Hydro-electric Power station.

Five fresh water sources were assigned to boundary nodes at the head of each short "river channel" which had a minimal depth 5 m and were connected to not less than 3 triangular elements. The discharge from all lower basin rivers was accumulated to a single river Nant, discharged at single point in southern part of Airds Bay.

To define rivers temperature T_R we estimate sea surface temperature T_0 from the upper-most temperature sensor deployed in the area (Saulmore point 9 m for hindcast runs, or sub-surface Access#11 thermistor chain available 4 times a day since December 2011) and adjust it toward the night air temperature T_A from the nearest weather station at 2 m height for positive T_A:

$$T_R = \begin{cases} 0.5 \cdot \ T_0 + T_A & , if\ T_A > 0 \\ T_0 & , if\ T_A \leq 0 \end{cases} \quad (3)$$

Finally zero-phase filter with Butterworth 7-point window was applied to T_R to create daily river temperature time series (**Fig. 5j**).

4.5 Initial (climatological) and boundary conditions

Monthly average 3D temperature and salinity fields were calculated using 82 CTD profiles from 8 standard RE stations approximately evenly distributed along the basin axis and obtained

during REES experiment in 1999-2001 (grey profiles **Fig**. **3**). This data for January and June were used to initialise the model.

Climatology of monthly coastal temperature and salinity profiles with 0.25° spatial resolution at standard levels were compiled by UK Hydrodraphic Office (UKHO). The nearest grid point data from UKHO climatology was re-interpolated linearly at the model open boundary points and vertical sigma-levels were initially used as the source of open boundary data for a series of sensitivity model tests in search for an optimal mesh. Maintaining the same initial T,S conditions at the open boundary would keep identical internal pressure gradients along the open boundary during the model run. To avoid this we firstly re-interpolate monthly T and S onto daily values. Secondly, after stable solutions were obtained, we found it necessary to have more accurate boundary conditions, which would allow nudging of the temperature and salinity not only back to initial conditions, but to more realistic open boundary values using the Blumberg/Kantha implicit gravity wave radiation conditions (Chen, 2006). In the absence of a full and frequent series of CTD profiles or the other (coarse) model output for the area in a given period of time, we constructed a temperature/salinity profiles with hourly resolution, adjusted to the tides in Ardmucknish bay and to the observed oscillations of sub-surface T and S values normalized to UKHO climatology from the upper instrument of the nearest monitoring station in Tiree Passage (Inall et al, 2009), located some 40 miles away from the model open boundary. Particularly in upper 5 m layer we introduced tidally-depended oscillations in salinity, varying in a range 26 –31 psu during the ebb phase, increasing toward 32.5 – 33.5 psu on the flood phase. These values correspond to the high resolution observations with AUV trials and short (3-4 days) moorings deployments in Ardmicknish bay in two seasons – in December 2009 and May 2010 (Boyd et al, 2011). For temperature variations a combination of data from subsurface Saulmore (9 m), Access 11 (0 m) and Foram (30 m) temperature loggers were used.

The latest model runs are based on the CTD casts, taken in November 2009 and April 2010 in the inner and lower basins, linearly distributed over model domain.

4.6 Meteo data and wind forcing

Meteo-forcing for FVCOM included the measured precipitation rate, atmospheric sea level pressure, air temperature at 2 m height, east-west and north south components of the winds at 10 m and solar radiation. The evaporation rate, short wave radiation and net heat flux, defined as a sum of short-wave, long-wave, sensible and latent heat fluxes, are calculated with standard bulk-formulae algorithms (Fairall et al 2003). FVCOM can incorporate wind forcing at the free surface in a traditional form of either direct wind stress or wind speed, which is converted to the stress at each time step and used to calculate the drag coefficient (Chen, 2006). Free-surface boundary data are automatically re-interpolated from relatively coarse meteo-grid to the model mesh (nodes for scalars and centroids for winds).

We used the hourly data from 5 coastal Met-Office weather stations from the Argyll region, separated by the distances 15-50 km: Dunstaffnage, Tiree Airport, Machrihanish, Islay-Port-Ellen and Lochgilphead. The solar radiation data are available only from Tiree and Dunstaffnge. Multiple gaps in the data sets were filled with a nearest neighbourhood algorithm. We applied simplified optimal interpolation/extrapolation technique with 20 km de-correlation spatial scale to distribute meteo-forcing data over the whole Firth of Lorn model area. Of course this approach in such a mountainous region with huge number (~1500) of large and small high islands and narrow channels is an essential over-simplification, especially for the wind field. More accurate compilation of the wind forcing data from only a few available observation points over the model domain is not a trivial challenge.

The regional weather forecasting model WRF with sufficient (1 km) horizontal resolution is currently at an early stage of development. The wind fields for winter 2010 in the region of interest were extracted from the first results of our WRF2.3 run and shown on **Fig. 2**(a,b). The steering effect of local topography and channels over the sea-lochs and glens is well captured by this sophisticated weather model, and opens a better way to force realistic oceanic shelf model applications in the future.

Section 5

Model Validation

5.1 Winds and the model velocity

Wind plays important role in fjord circulation especially in mountainous regions. Tangential wind stress applied to the ocean upper layers produce vertical shear in velocity field. High correlation (0.65) was found between near-surface currents and along channel winds during two month series of observations with massive mooring arrays and profiling current meters in Knight Inlet, British Columbia (Baker Pond, 1995). Comparison of measured wind speed and model response with wind induced near-surface currents is the convenient basic test of model performance. For comparison we plot a time series of the measured along-axis wind component, shown on **Fig.12 a** and the along axis component of sea surface velocity, extracted from the model centroid nearest to Hypox mooring site in the inner basin of loch Etive (**b**). The correlation between daily averaged wind and residual velocity is the highest (0.81) in the near-surface layer with the range [0.75-0.85] at the 95% confidence level. As expected the model response to wind forcing reduces with depth and correlation reverses in sign at depths of 25-35 m (**Fig.11c**). The near surface values of the correlation coefficients are close and even higher than the correlation value 0.65 reported by Baker and Pond (1995) in a similar basin. From this we can conclude that the winds applied to the model produce the correct surface stress during half a year model run.

5.2. Pressure measurements and model surface elevation

Quantitative comparisons based on regression analyses and the index of agreement is given in **Table 5**. Index of agreement (*d*) is a model skill introduced by Wilmott (1981) can be defined as:

$$d = 1 - \frac{\sum_{i=1}^{N}(M_i - O_i)^2}{\sum_{i=1}^{N}(M_i - \bar{O} + O_i - \bar{O})^2} \quad (4)$$

where *M* and *O* are the modelled and observed variables, $\bar{O}$ is whole time mean of *O*, and *N* is the number of data points. The *'perfect'* and *'excellent'* agreement between the model calculations and observations are obtained when skill close to one and complete disagreement gives a skill near zero.

From **Table 5** we can conclude the sea level simulation skill is high for two stations available for comparison. The lowest correlation coefficient is 0.84 and the lowest index of agreement is 0.88. The maximum RMS error is 0.42 and 0.39 m, which is about 15% and 12 % of the sea level variation range at Hypox and Airds Bay mooring sites from pressure records. This gives us confidence that the model is capable to simulate the water elevation with high accuracy.

5.3. Model validation and currents measurements

We found that model required approximately 2 days of spin-up period to allow the density field to adjust over the model domain when the velocity field is applied with tidally driven sea level oscillations along the open boundary from a state of rest. We also used a ramping period (12 hours) which gradually increases the values of external forcing data to its final range. The only available current meter data from loch Etive during the period of observation is the subsurface conventional Aanderaa Seaguard, deployed at the Hypox mooring site in the inner basin and a short (3 days) RDI ADCP data set form the moorings deployed in Ardmucknish bay in May 2010 (Boyd et al, 2010). The currents are generally overestimated (30-50%) by the model in comparison with the few accessible current measurements. The model tidal ellipses (M_2) demonstrate general agreement with the results of measurements, but the minor axis of model ellipses is wider, in comparison with the ellipses from the moorings.

5.4 Temperature and salinity fields

The best model performance is achieved with the surface elevation for both short and long term runs. Among other parameters the temperature reconstructions at Saulmore and Forma points demonstrate similar high skills, shown in **Table 6.** The lowest correlation coefficient is 0.98 and the lowest index of agreement is 0.93. The maximum RMS error is 1.01 and 0.69 °C

which is about ~15 % of the whole temperature range at the mooring sites. The model is accurate in the simulation of the water temperature at least in the upper 10-30 m layer. Three-dimensional distributions of typical mid-winter temperature and salinity distribution can be derived from a combination of seas-surface maps (**Fig. 16**) and vertical transects along Loch Etive axis (**Fig. 17**). The seasonal cycle in the external forcing data is well represented by the model in the upper layer up to the depth 30 – 50 m, as show in the temperature time series (**Fig. 14**). No substantial drifts away from observed values of temperature and salinity were found for a 7 month long calculation. We conclude that the model is able to generate the main seasonal signal in the temperature and salinity fields in response to consistent variations at open and surface boundaries. High frequency oscillations in salinity are closely linked with fluctuations in the fresh water supply into the model domain. Thin layers of fresh waters periodically spread from rivers over the basin and quickly (within a few hours) become mixed with the underlying layers.

Long-term fluctuations in salinity field are generally reproduced with less accuracy (**Fig. 15**), while the range of variations is close to observed values (± 1 psu). The thickness of both thermo- and haloclines is generally greater in the model, than seen in the CTD observations. Lack of initial and boundary data exposed real difficulties for the model to reproduce the winter 2010 overturning events, a subject we now turn to in greater detail.

5.5 Simulation of renewal event

Improvements in reproducing of the vertical T,S structure during an renewal eventwas achieved by increasing the vertical resolution with a 31 layer model, developed specifically for a case study of the summer overturning event. The temperature and salinity vertical distribution across the Bon-Awe sill at the final stage of a renewal event at the end of June 2010 are shown in **Fig. 18**. The evolution of vertical thermo-haline structure during one flood-ebb cycle is shown by a series of snapshots with two hour intervals. The corresponding patterns of sea-surface velocity filed are shown at **Fig.19**.

The west side of the basin (Airds bay) is filled with warm and more saline waters, which are blocked above the sill with fresher and colder waters brought with the ebb tide from the inner basin (east side) at the beginning of the process (13:59). With the reverse of the tide (start of flood phase, 16:00) warm and saltier waters aspired from the layers 20-30 m upward and occupied the top of the sill area. During the next step (2 hours) these waters begin to sink down along the eastern slope of the sill. This gravity current did not separate from the bottom and eventually delivered a portion of new heavy, salty and warm waters to the deepest part of the inner basin. Intensive non-linear dynamical structures formed on a lee-side of the sill as indicated by bends in isotherms and isohalines with vertical amplitude 20-30 m and sharp horizontal gradients (2°C and 3 psu per 300 m). The duration of the modelled overturning event was twice as long (~20 tidal cycles) than the observed one (10). However the main features of the process were captured in this simulation.

The HYPOX program monitors the necessary conditions for overturning (minimal fresh water supply due to low precipitation and low discharge of river Awe, favourable down-fjord wind, falling in Atmospheric pressure, approaching spring tide). Nevertheless all attempts to simulate the renewal event without information about the temperature and salinity distribution at the model open boundary failed. To fill the lack in the information about open boundary conditions for the Loch Etive domain, another regional model of the adjacent basin (Firth of Lorn) was required.

A new finite volume coastal ocean model for western Scotland has been developed for the EC project ASIMUTH to study Harmful Algae Blooms. This model has slightly coarser resolution with a minimal horizontal scale of 49 m, 25001 elements and 11 vertical layers. We ran the first spin-up tests of the Firth of Lorn model initially without information at the open boundary, but with realistic meteorological and river discharge forcing for the year 2010. The latest version of this model has a regular open-boundary fed from another near-real-time North-Atlantic 2x2 km model (ROMS) developed by the ASIMUTH partners at the Marine Institute Ireland (Kieran Lyon), which itself is forced by MyOcean/Mercator near-real-time and prognostic Atlantic models (NEMO) with 12 km horizontal resolution. Two snapshots of sea surface density from this model for summer 2011 zoomed to the entrance to Loch Etive are shown at **Fig. 2 c, d.**

The results from the Firth of Lorn model have been applied to a summer 2010 simulation of Loch Etive. Time-series (Temperature, Salinity and Potential Density) from the nearest node to RE8 station for summer 2010 and 2011 are shown on **Fig. 20 a,b**. This location is close the open boundary of the Loch Etive Model, approximately one mile west of Ardmucknish Bay. The difference in the sea water temperature was minor, while the most prominent contrast found was in the salinity field. According to the model in summer 2010 a pool of high salinity water (S > 33.5 psu) was formed in the whole adjacent area of Firth of Lorn. A thin layer (2-8 m) of fresher water appears only in July 2010 (after heavy rain), slowly increasing in depth since that time corresponding to the accumulative precipitation over the basin. In contrast, in 2011 the model demonstrate that the whole Firth of Lorn basin becomes much less saline (S<33.5 psu) and the thickness of halocline increased dramatically to a depth of 20 - 30 m.

For both summer 2010 and 2011 there was available data of weekly CTD casts at LY1 station in the Lynn of Lorn, close to the North-Western segment of the model open boundary, thanks to monitoring activity by K. Davison (**Fig. 20 c,d**). Our suggestion received clear confirmation by comparison of the model data and direct measurements in the area. A pool of dense water clearly formed near Ardmucknish bay in June 2010. Finally, this is the most important and necessary condition required to trigger the renewal event in the inner basin of Loch Etive, which was successfully simulated by combining the two models.

Section 6

Discussion and Conclusions

The first winter overturning event in 2010 was driven mostly by a decrease in sea water temperature in combination with decreased air temperature, favourable winds and reduced fresh water input, which led to a decrease in density stratification at the entrance to the loch. The summer overturning event was mainly caused by relative draught, which resulted in a significant reduction of the fresh water supply to the loch itself and to the adjacent coastal sea, thus weakening coastal stratification.

The results of observations off both the winter and summer 2010 overturning events demonstrate the highest contribution from tidally exaggerated flow over the sill along (in strong connection) with density-driven circulation and wind-driven entrainment. That is consistent to the conclusions derived from 3-layer box model runs (Gillibrand et al, 2012) for the spring overturning that took place in 2000.

Edwards and Edelsten (1977) suggested previously that the number of renewal events in Loch Etive was reduced by a factor of two in 1960-1970s as a result of the delaying of discharge of the fresh waters accumulated earlier in the catchment area (Loch Awe) and further damping by the hydro-electric station during spring/summer dry spells. In winter and spring 2010 the precipitation over the area was so low that a discharge of the accumulated waters by hydro-electric scheme dropped to the minimum allowable level. Overturning then happened when this anthropogenic factor was combined with the four key natural factors:

- favourable winds (down the fjord),giving rise to increased compensational underflow of saltier/colder and heavier waters toward entrance and further up the loch;
- raising sea level due to the invers barometer effect, which increased the vertical cross-sectional area over the sills, which, in turn, increased the volume transport, and thus both the amount of aspired dense water delivered to inner basin at flood phase, and the amount of light surface waters removed from the sill area during the ebb tide;
- the intensity of barotropic flow over the sills was amplified due to increase in the amplitude of the sea level undulation on the approach of a spring tide;
- pool of dens waters was formed at the entrance to the Loch, and the density of the upper layer in Ardmucknish bay was higher than the density of stagnant waters in deep inner basin.

One mean to increase deep basin renewal frequency could be suggested from this analysis. When all natural factors discussed above occur there is a possibility of triggering an overturning event by manually reducing of fresh water discharge of the hydro-electric power station for a period of several days. The loss in electric energy production could be compensated immediately by releasing the withheld water after the renewal event has occurred. This early alert system would require the installation of two moored monitoring stations, each equipped with at least 2

sets of CTD sensors in the upper and bottom layer (one in the inner basin, and the other at loch entrance in Ardmucknish Bay) with real-time data transmission (mobile sms, iridium-satellite or cabled). Capability of these type installations has been successfully demonstrated within the HYPOX project (delayed mode mooring in Airds bay and cabled mooring next to Glen Noe) in 2010-2011.

Acknowledgments

This research was carried out within the HYPOX project EC Grant #226213. The authors are grateful to R/V Calanus crew and SAMS PSIT team (J. Beaton, E. Dumond, C. Griffiths, J. Montgomery). We are thankful for the data used in this research including temperature loggers from NERC Diving Unit (M. Sayer), ADCP and SBE moorings data for AUV trials in Ardmucknish Bay (T. Boyd and M. Inall) and the data of Acesess-11 thermistor chain (K. Jackson), side-scan and multibeam bathymetry (S. Gontarek and J. Howe); river Awe discharge data of Scottish and Southern Energy; BADC for meteodata; Ocean2025 and shelf-sea consortium for access to HECToR super-computer and FVCOM code from C. Chen (SMAST/UMASSD).

Literature

Anderson, J. J. and Devol, A. H. 1973. Deep water renewal in Saanich Inlet, an intermittently anoxic basin.Estuarine & Coastal Marine Science I, 1-10.

Arneborg L, Liljebladh B. 2001.The internal seiches in Gullmar Fjord. Part II: Contribution to basin water mixing. J. Phys. Oceanogr., 31, 2567-2574.

Arneborg, L., 2004. Turnover times for the water above sill level in Gullmar Fjord. Continental Shelf Research, 24, 443-460.

Austin, W. E. N. and M. E. Inall, 2002. Deep-water renewal in a Scottish fjord: temperature, salinity and oxygen isotopes. Polar Research 21(2): 251-257

Baines, P. G., 1995, Topographic Effects in Stratified Flows. Cambridge, Cambridge University Press, XVI, 482 pp.

Baker, P., Pond, S., 1995. The low-frequency residual circulation in Knight Inlet, British Columbia. J. Phys. Oceanogr. 25, 747-763.

Bell, W. H. 1973. The exchange of deep water in Howe Sound basin. Marine Sciences Directorate, PacificRegion Environment Canada, Report 73(13), 35.

Boyd, T., M. Inall, E. Dumont, and C. Griffiths (2010), AUV-based observations of mixing in the tidal outflow from a Scottish Sea Loch, 2010 IEEE-OES Autonomous Underwater Vehicles (AUV), ISBN 978-1-61284-979-9. www.rocklandscientific.com

CEH report 2010, Hydrological Summary for the United Kingdom, Available at www.ceh.ac.uk/data/nrfa/nhmp/hs/pdf/HS_201012.pdf (accessed 18 January 2012)

Chen, C., Beardsley, R.C., Cowles, G., 2006. An Unstructured Grid Finite-Volume Coastal Ocean Model: FVCOM User Manual. University of Massachusetts-Dartmouth, USA. Available from: http://fvcom.smast.umassd.edu/FVCOM/index.html

Chen, C., G. Gao, J. Qi, A. Proshutinsky, R. C. Beardsley, Z. Kowalik, H. Lin, and G. Cowles, 2009. A new high-resolution unstructured grid finite volume Arctic Ocean model (AO-FVCOM): An application for tidal studies, J. Geophys. Res., 114, C08017, doi:10.1029/2008JC004941.

Chen, C., H. Liu, and R. C. Beardsley, 2003. An unstructured, finite volume, three-dimensional, primitive equation ocean model: Application to coastal ocean and estuaries, J. Atmos. Oceanic Technol., 20, 159-186.

Cowles, G., 2008. Parallelization of the FVCOM Coastal Ocean Model, Int. J. High Perform. Comput. Appl., 22(2), 177 - 193, doi:10.1177/1094342007083804.

Cushman-Roisine, B., Tverberg, V., Pavia E.G. 1989.Resonance of internal waves in fjords: A finite-difference model. J. of Marine Res., 47, 547-567.

Dickson, R. R. 1973.The prediction of major Baltic inflows. Deutsche Hydrographische Zeitschrift, 26,97-105.

Edwards, A. and D. J. Edelsten, 1976. Control of Fjordic Deep Water Renewal by Runoff Modification / Réglage du renouvellement des eaux profondes des fjords en utilisant un modèle qui effectue une modification du régime de l'écoulement. Hydrological Sciences Bulletin, 21:3, 445-450

Edwards, A. and D. J. Edelsten, 1977. Deep-Water Renewal of Loch Etive - 3 Basin Scottish Fjord. Estuarine and Coastal Marine Science 5(5), 575-595.

Edwards, A., Sharples, F. 1986. Scottish Sea Lochs: A Catalogue. Scottish Marine Biological Association, Oban, U.K. 109 pp..

Fairall, C.W., E.F. Bradley, J.E. Hare, A.A. Grachev, and J.B. Edson. 2003. Bulk parameterization of air sea fluxes: updates and verification for the COARE algorithm, J. Climate, 16, 571-590.

Farmer D.M. and H.J. Freeland. 1983. The physical oceanography of fjords. Progress in Oceanography. 12(2):147-220.

Farmer, D.M., Armi,L., 1999. Stratifed flow over topography: The role of small scale entrainment and mixing in flow establishment. Proceedings of the Royal Society of London, A455:3221-3258.

Foreman M.G.G., Czajko P., Stucchi D.J., Guo M., 2009. A finite volume model simulation for the Broughton Archipelago, Canada. Ocean Modelling, 30:29-47.

Foreman, M.G.G., Stucchi, D.J., Zhang, Y., Baptista, A.M., 2006. Estuarine and tidal currents in the Broughton Archipelago. Atmos. Ocean 44, 47-63.

Gillibrand, P. A., A. G. Cage, et al. 2005. A preliminary investigation of basin water response to climate forcing in a Scottish fjord: evaluating the influence of the NAO. Continental Shelf Research 25(5-6): 571-587.

Gillibrand, P. A., Inall, M. E., Portilla E. and P. Tett. 2012. A Box Model of the Seasonal Exchange and Mixing in Regions of Restricted Exchange: Application to Two Contrasting Scottish Inlets. Environmental Modelling and Software (submitted).

Gillibrand, P. A., Turrell, W. R., Elliott, A.J. 1995. Deep-Water Renewal in the Upper Basin of Loch Sunart, a Scottish Fjord. J. Phys. Oceanogr., 25, 1488-1503.

Gillibrand, P. A., W. R. Turrell, et al. 1996. Bottom water stagnation and oxygen depletion in a Scottish sea loch. Estuarine Coastal and Shelf Science 43(2): 217- 235.

Gilmartin, M. 1962. Annual cyclic changes in the physical oceanography of a British Columbia fjord.J. of the Fisheries Research Board of Canada 19, 921-974.

Haney, R.L., 1991. On the pressure gradient force over steep topography in sigma coordinate ocean models. J. Phys. Oceanogr. 21, 610-619.

Howe J., Overnel, J., Mark E. Inall, M.E., and Wilby A.D., 2001 A side-scan sonar image of a glacially-overdeepened sea loch, upper Loch Etive, Argyll, Scottish Journal of Geology, 37, 3-10.

Howe, J. A., Overnell, J., Inall M.E., and A. D. Wilby, 2001. A side-scan sonar image of a glacially-overdeepened sea loch, upper Loch Etive, Argyll. Scottish Journal of Geology, 37:3-10, doi:10.1144/sjg37010003.

Howe, J.A., Shimmield, T.M., Austin, W.E. N and Longva O. 2002 Post-glacial depositional processes in a glacially-overdeepened sea loch, upper Loch Etive , Western Scotland. Marine Geology,185:417-433

Inall M.E., Gillibrand P., Griffiths C.R., MacDougal N. and Blackwell K. 2009. On the oceanographic variability of the North-West European Shelf to the West of Scotland. Journal of Marine Systems ,77(3):210-226.

Inall, M. E. 2005. Turbulence measurements in fjords. Marine Turbulence: Theories, Observations and Models. H. Z. Baumert, J. H. Simpson and J. Sunderman. Cambridge, Cambridge University Press. 1: 340 - 345.

Inall, M. E. 2009. Internal wave induced dispersion and mixing on a sloping boundary. Geophys. Res. Lett., 36, L05604, doi:10.1029/2008GL036849.

Inall, M., Cottier, F., Griffiths, C., and T. Rippeth. 2004. Sill dynamics and energy transformation in a jet fjord, Ocean Dynamics, 54:307-314.

Inall, M., Gillibrand P., 2010. The Physics of mid-Latitude Fjords: A Review. Geological Society, London, Special Publications 2010, 344:17-33; doi:10.1144/SP344.3

Inall, M., Rippeth, T., Grifiths, C. and P. Wiles. 2005. Evolution and distribution of TKE production and dissipation within stratified flow over topography. Geophys. Res. Letters, 32:L08607, doi:10.1029/2004GL022289.

Ivchenko, V. O., Danilov, S., Sidorenko, D., Schroeter, J., Wenzel, M., and Aleynik, D. L. 2008. Steric height variability in the Northern Atlantic on seasonal and interannual scales, J. Geophys. Res., 113, C11007, doi:10.1029/2008JC004836.

Loh, P. S., A. E. J. Miller, et al. 2008. Assessing the biodegradability of terrestrially-derived organic matter in Scottish sea loch sediments." Hydrology and Earth System Sciences,12 (3), 811-823.

Malcolm, S.J., Price, N.B., 1984. The behaviour of iodine and bromine in estuarine surface sediments. Mar. Chem., 15, 263–271

Magill S., Black K., Kay D., Stapleton C., Kershaw S., Lees D., Lowther J., Francis C., Watkins J. & Davies C. 2008. Risk factors in shellfish harvesting areas. Final Project Report, prepared for Scottish Aquaculture Research Forum.SARF013/SAMS report No 256. Scottish Association for Marine Science, Centre for Research into Environment and Health and CEFAS. Available at http://www.sarf.org.uk/Project Final Reports/SARF013 - RISK_FACTORS_IN_ SHELLFISH_HARVESTING_AREAS - 23June2008.pdf (accessed 18 January 2012)

McKee, D., A. Cunningham, et al. 2002. Optical and hydrographic consequences of freshwater run-off during spring phytoplankton growth in a Scottish fjord. *Journal of Plankton Research*, **24** (11), 1163-1171.

Mellor, G.L., Ezer, T., Oey, L.-Y., 1994. The pressure gradient conundrum of sigma coordinate ocean models. J. Atmos. Oceanic Technol. 11, 1126-1134.

Mellor, G.L., Yamada, T., 1982. Development of a turbulent closure model for geophysical fluid problems. Rev. Geophys. Space Phys. 20, 857-875.

Miller, J. 2002. The dam builders: power from the glens. Edinburgh, Birlinn Ltd, P. 256.

Nerem, R. S. et al. 2010. Estimating Mean Sea Level Change from the TOPEX and Jason Altimeter Missions. Marine Geodesy 33: 435-446.doi:10.1080/01490419.2010.491031.

Nørgaard-Pedersen, N., W.E.N. Austin J.A. Howe, T. Shimmield. 2006 The Holocene record of Loch Etive , western Scotland: Influence of catchment and relative sea level changes. Mar. Geology. 228, 55-71.

Overnell, J., T. Brand, et al. 2002. Manganese dynamics in the water column of the upper basin of Loch Etive, a Scottish fjord. Estuarine Coastal and Shelf Science 55(3): 481-492.

Overnell, J., S. M. Harvey, et al. 1996. A biogeochemical comparison of sea loch sediments. Manganese and iron contents, sulphate reduction and oxygen uptake rates. Oceanologica Acta 19(1), 41-55.

Paulson, A., S. Zhong, and J. Wahr. Inference of mantle viscosity from GRACE and relative sea level data, 2007.Geophys. J. Int. 171, 497-508. doi: 10.1111/j.1365-246X.2007.03556.x

Portilla, E.and Tett P. 2008, Estimation of fresh water runoff into a fjord: Time series analysis versus a mechanistic modelling approach. Manuscript., P.1-36.

Rippeth, T.P. and Simpson, J.H. 1996.The frequency and duration of episodes of complete vertical mixing in the Clyde Sea. Continental Shelf Res., 16(7), 933-947.

Saelen, O. H. 1947. Temperature variations and heat transport in the Nordfjord. Bergens Museums Arbok, Naturvitenskapelig Rekke, 6, 1-28.

Smagorinsky, J., 1963. General circulation experiments with the primitive equations. I. The basic experiment. Monthly Weather Review 91 (3), 99e164.

Stashchuk, N., Inall, M. et al. 2007. Analysis of supercritical stratified tidal flow in a Scottish Fjord. J. of Phys. Oceanography 37(7): 1793-1810.

Stigebrandt, A. 1976.Vertical diffusion driven by internal waves in a Sill Fjord. J. Phys. Oceanogr., 6:486-495.

Stigebrandt, A. 1977. On the effect of barotropic current fluctuations on the two-layer transport capacity of a constriction. J. Phys., Oceanogr., 7, 118-122.

Stigebrandt, A., 1980. Some aspects of tidal interaction with fjord constrictions. Estuarine and Coastal Marine Science, 11, 151-166.

Stigebrandt, A., 1981. A mechanism governing the estuarine circulation in deep, strongly stratified fjords.Estuarine Coastal and Shelf Science, 13,197-211.

Stigebrandt, A., 1999. Resistance to barotropic tidal flow in straits by baroclinic wave drag. Journal of Physical Oceanography, 29, 191-197.

Stigebrandt, A., 2001. FjordEnv - A water quality model for fjords and other inshore waters. Gothenburg University Report, Sweden, 41pp.

Stigebrandt, A., Aure, J., 1989. Vertical mixing in the basin waters of fjords. J. Phys. Oceanogr., 19, 917-926.

Wilding, T. A., Hughes, D. J., Black, K. D., 2005. The benthic environment of the North and West of Scotland and the Northern and Western Isles: sources of information and overview. Report 1 to METOC. Scottish Association for Marine Science, Oban, Scotland.

Wilmott, C.J., 1981. On the Validation of Models. Phys. Geogr. 2, 184 – 194.

Wood, B.J.B., Tett, P.B., Edwards, A., 1973. An introduction to the phytoplankton, primary production and relevant hydrography of Loch Etive. J. of Ecology, 61 pp. 569-585

Xing J., Davies A. M., 2009. Influence of bottom frictional effects in sill regions upon lee wave generation and implications for internal mixing. Ocean Dynamics. 59:837-861.

Young, A., 2006. Stream flow simulation within UK ungauged catchments using a daily rainfall-runoff model, Journal of Hydrology, 320, 155-172.

Figures

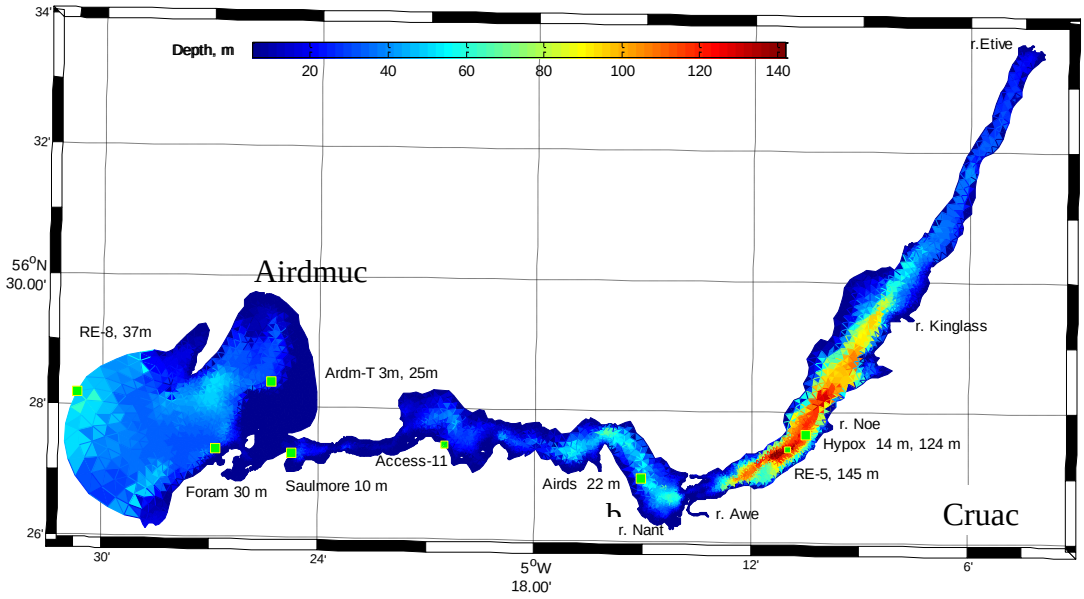

Figure 1. Bathymetry of Loch Etive based on combined data set of Admiralty Charts 1861 updated by echo-sounding in 1971, side-sonar survey 2000 (courtesy of S. Gontarek), and multi-beam surveys 2010 and 2011 (J. Howe, pers. com.). Location of 5 main rivers and REES CTD stations (RE8 and RE5), and various mooring sites is also shown with green squares: Hypox mooring RCM-11 at 14 m and RDCP-600 at 124 m; Airds bay – SBE16, temperature loggers at Foram and Saulmore point, and SBE-37 IM mooring in Ardmucknish bay at depth 3 m and 25 m, Acsess-11 sub-surface thermistor chain site.

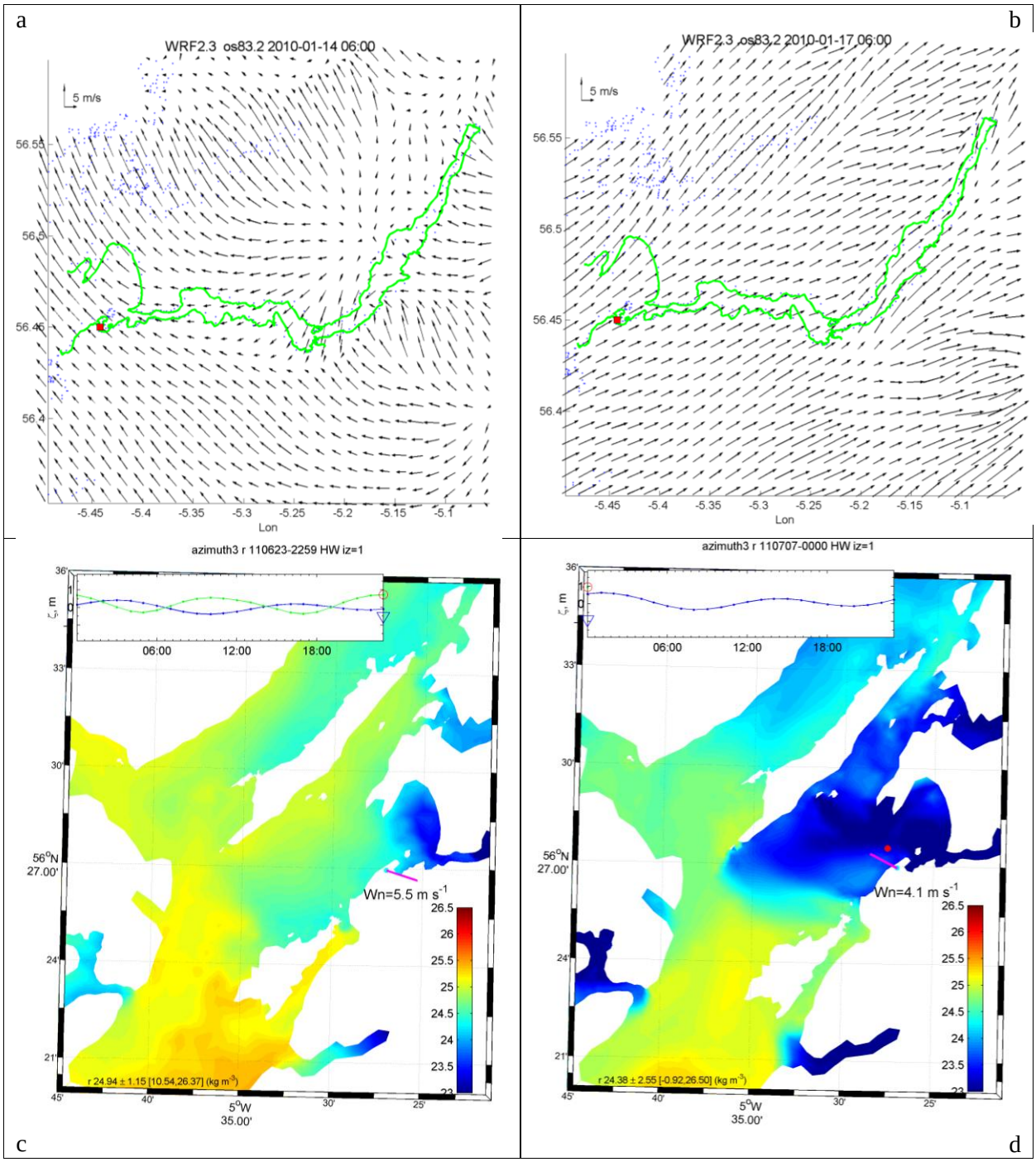

Figure 2. Typical wind patterns over the area from Weather Regional Forecast model *WRF3.2* run at 1x1 km grid, *os83.2*, *Jan 2010, 14$^{06:00}$and 17$^{06:00}$*(**a,b**).Tunnelling effect is clearly recognizable along the Loch Etive axis. Red squares refer to the locations of Dunstaffnage Weather Station (DWS), Bonawe sill and Hypox mooring site. Two distinct sea surface density patterns in the firth of Lorn from the coarse resolution *Fvcom* model run for ASIMUTH domain, illustrate high correlation with the wind field dominate direction at DWS: **c**) from NW and **d**) from SE. For the open boundary we used the 3-hourly output of NE-Atlantic ROMS 2.5 km Irish Marine Institute operational model (http://www.marine.ie) and 1-h local meteo-data (BADC) for summer 2011.

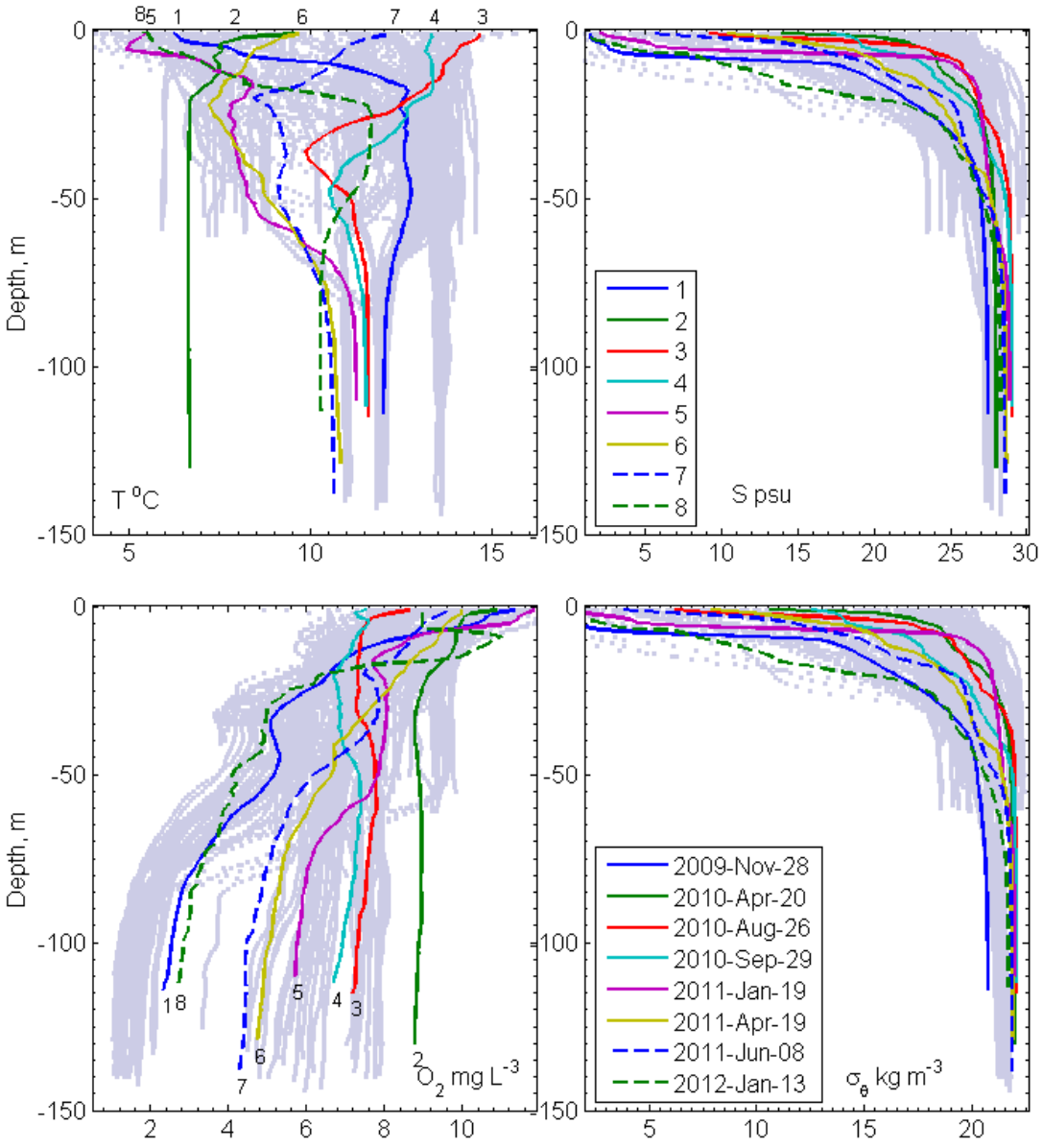

Figure 3.1 Historical vertical profiles of Temperature (a), Salinity (b), Dissolved Oxygen (c) and Potential Density (d) from RE1-8 CTD stations along the axis of the Loch Etive obtained in 1999-2001 with REES *experiment* (The Restricted Exchange Environments) are shown in grey. Vertical profiles from the inner basin measured during HYPOX monitoring program 2009-2012 are shown in colour. The renewals events took place between CTD surveys 1 (blue) and 2 (green), and between 2 and 3(red).

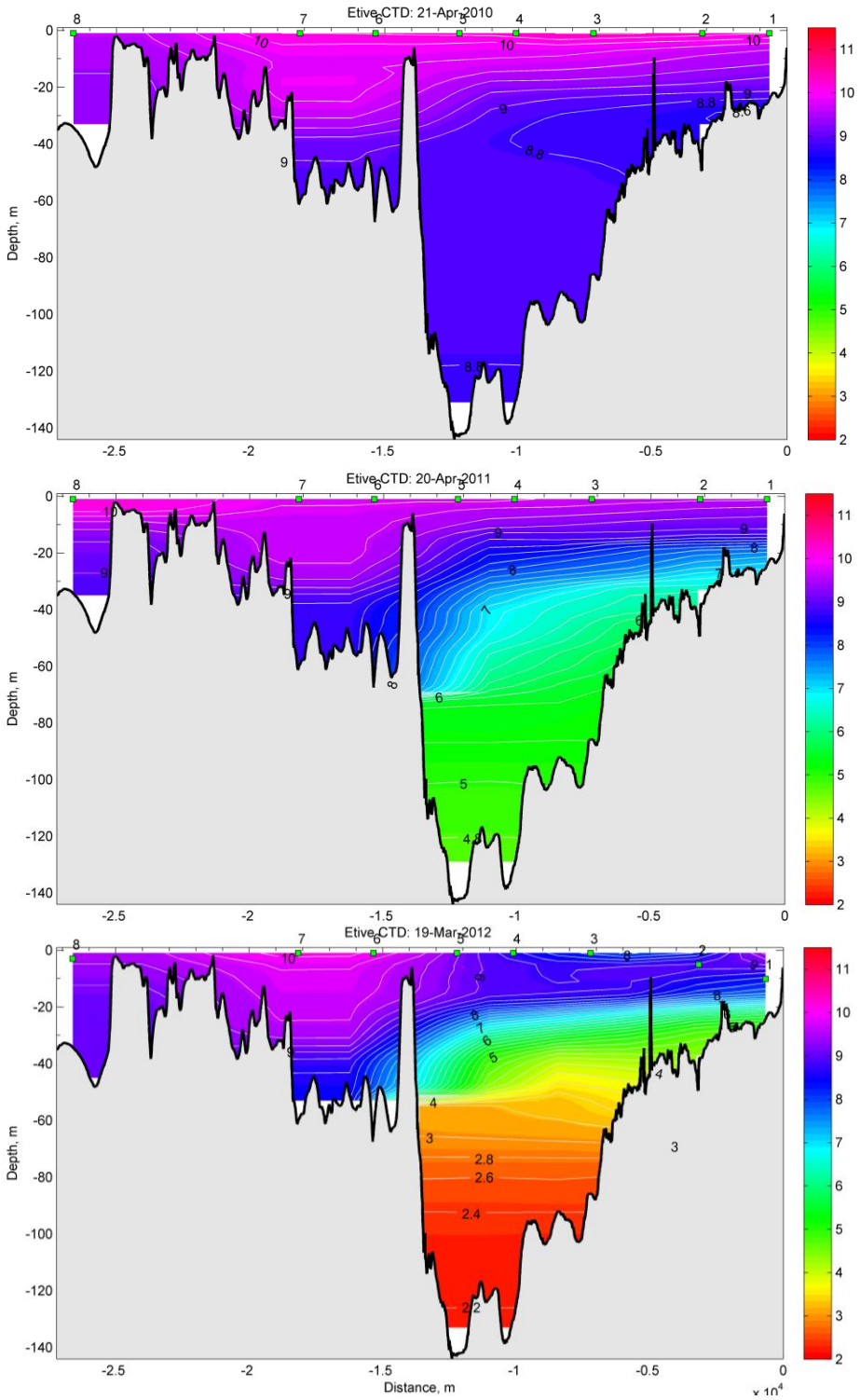

Figure 3.2. Vertical distribution of Dissolved Oxygen (mg L^{-1}) from RE1-8 CTD stations (SBE) along the axis of the Loch Etive obtained in April 2010, two month after the 2nd renewal (a) and in April 2011, ten month after the 3rd renewal (b), and in March 2012 (c).

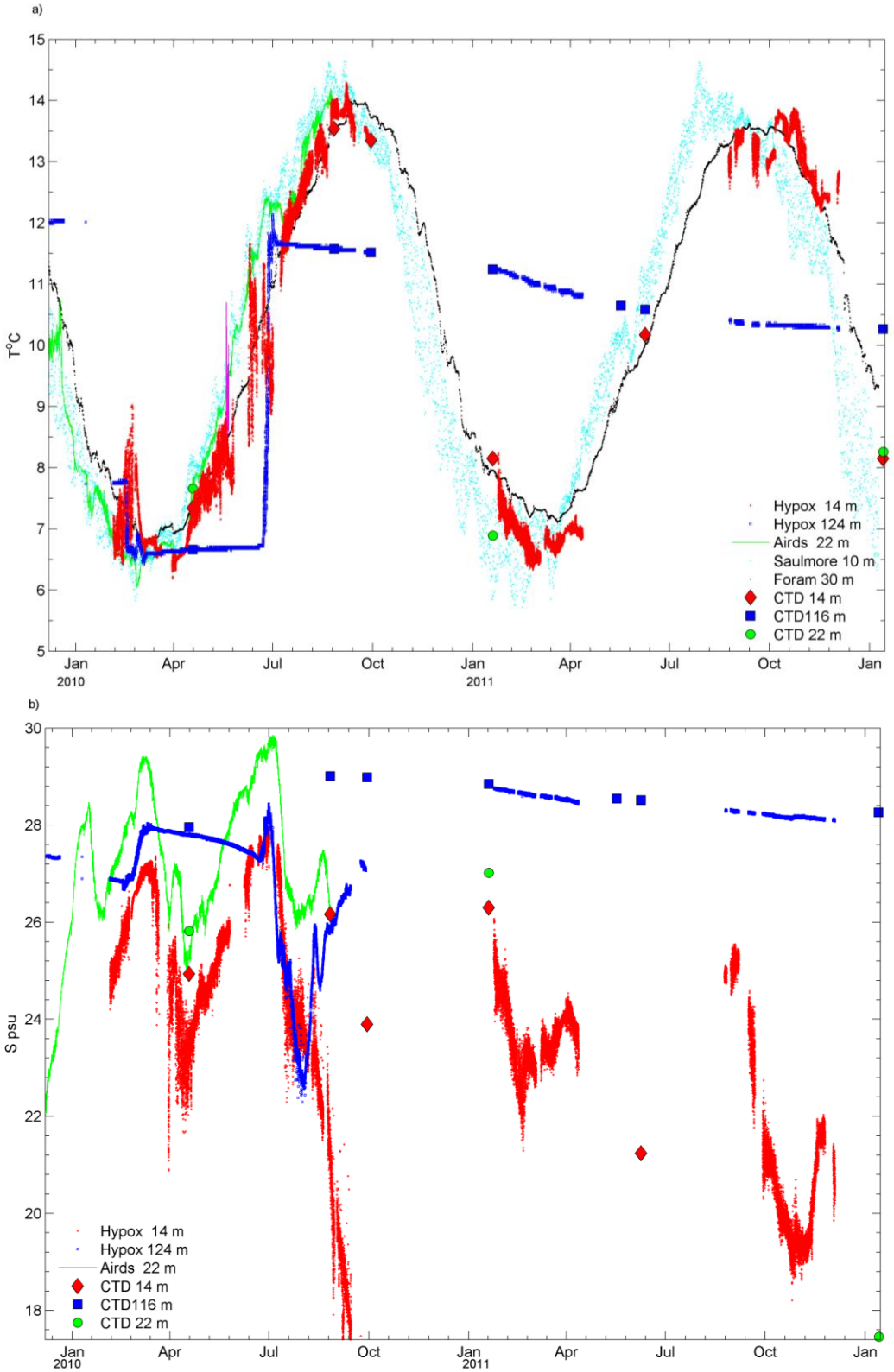

Figure 4a,b. Temperature, ºC (a) and Salinity (b) timeseries from mooring sites deployed in 2009/2011 in the upper (Hypox) and lower basins (all the others) of Loch Etive. CTD cast values at the same depth are also shown.

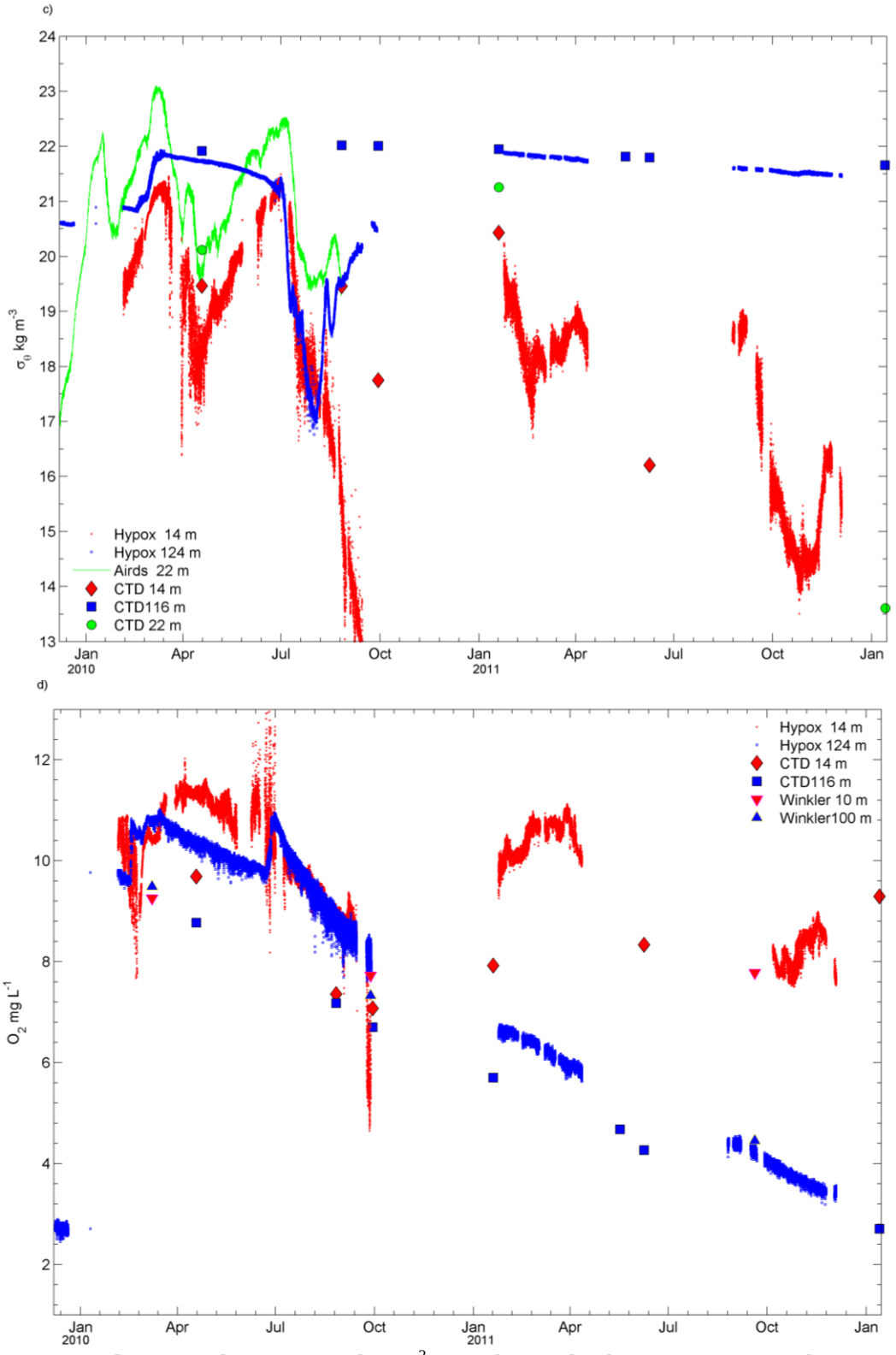

Figure 4c,d. Potential Density in kg m^{-3}(c) and Dissolved Oxygen converted to mg·L^{-1} from Aanderaa Optode(d), CTD SBE Oxygen sensors and Winkler O_2 samples at Hypox mooring site.

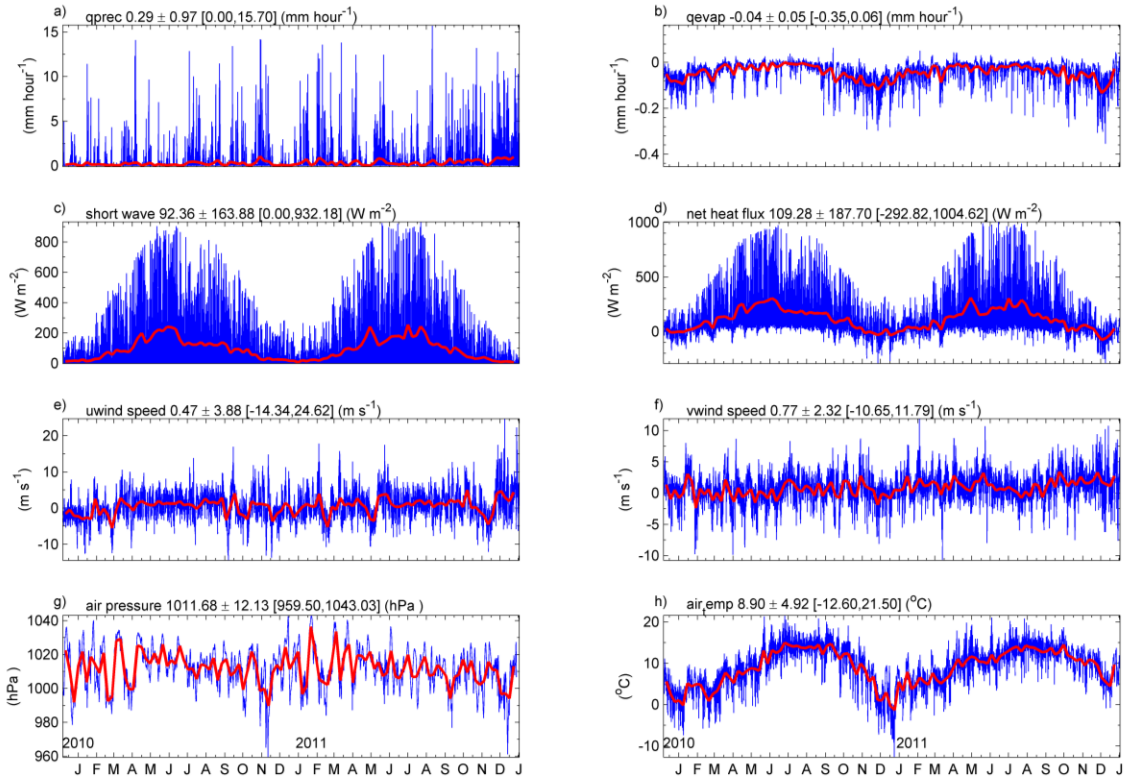

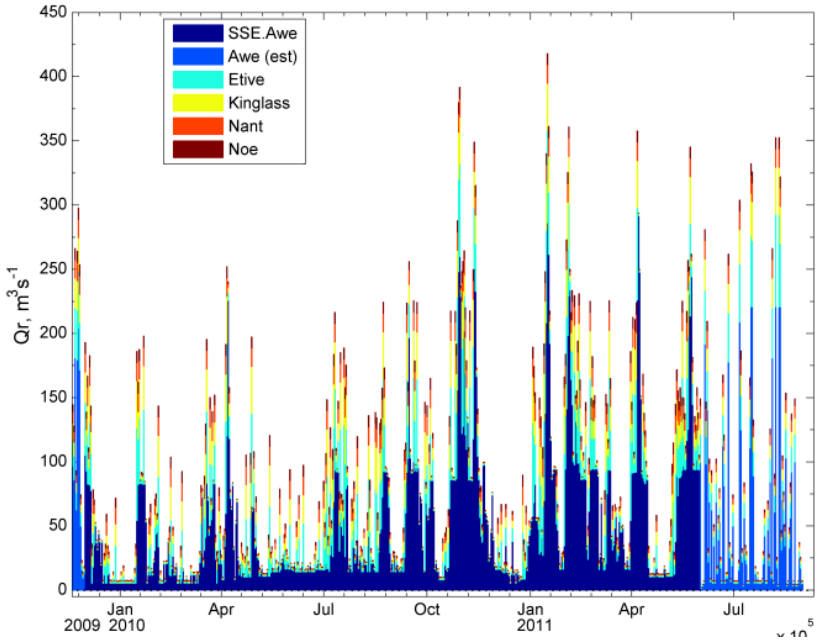

Figure 5. The annual cycles of meteorological parameters from Dunstaffnage Weather Station (Met-Office BADC ukmo-midas) with hourly resolution (blue) and weekly running-average (red) for period 2009/12 – 2011/12: **a**) precipitation, **b**) evaporation, **c**) short wave radiation, **d**) net heat flux, **e**) east-west and **f**) north-south wind components, **g**) air pressure at the sea level and **h**) air temperature. The average, standard deviation and the range for each parameter are shown above the graphs. The measured discharge rate for river Awe, provided by Scottish and Southern Energy (SSE) for 2009-June 2011 (deep blue), combined with fresh water input for major rivers, estimated using precipitation rates, catchment areas end evapo-transpiration factor (**i**).

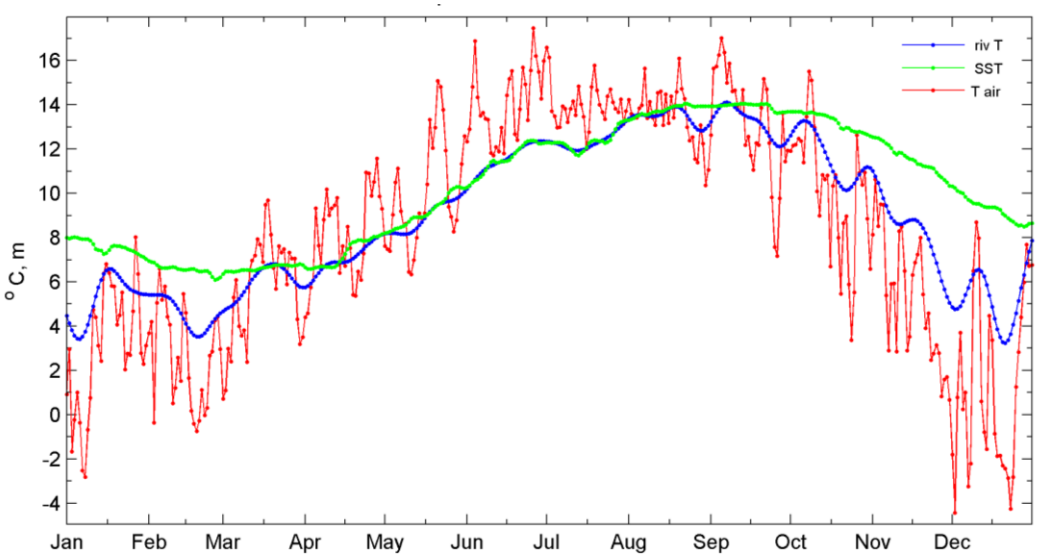

Figure 5 (continue). Time series of night air temperature at 2 m in Dunstafffnage (red), daily average sea surface temperature in nearby area (green), and reconstructed with formula 3 (p.20) rivers temperature (blue) for 2010 (**j**).

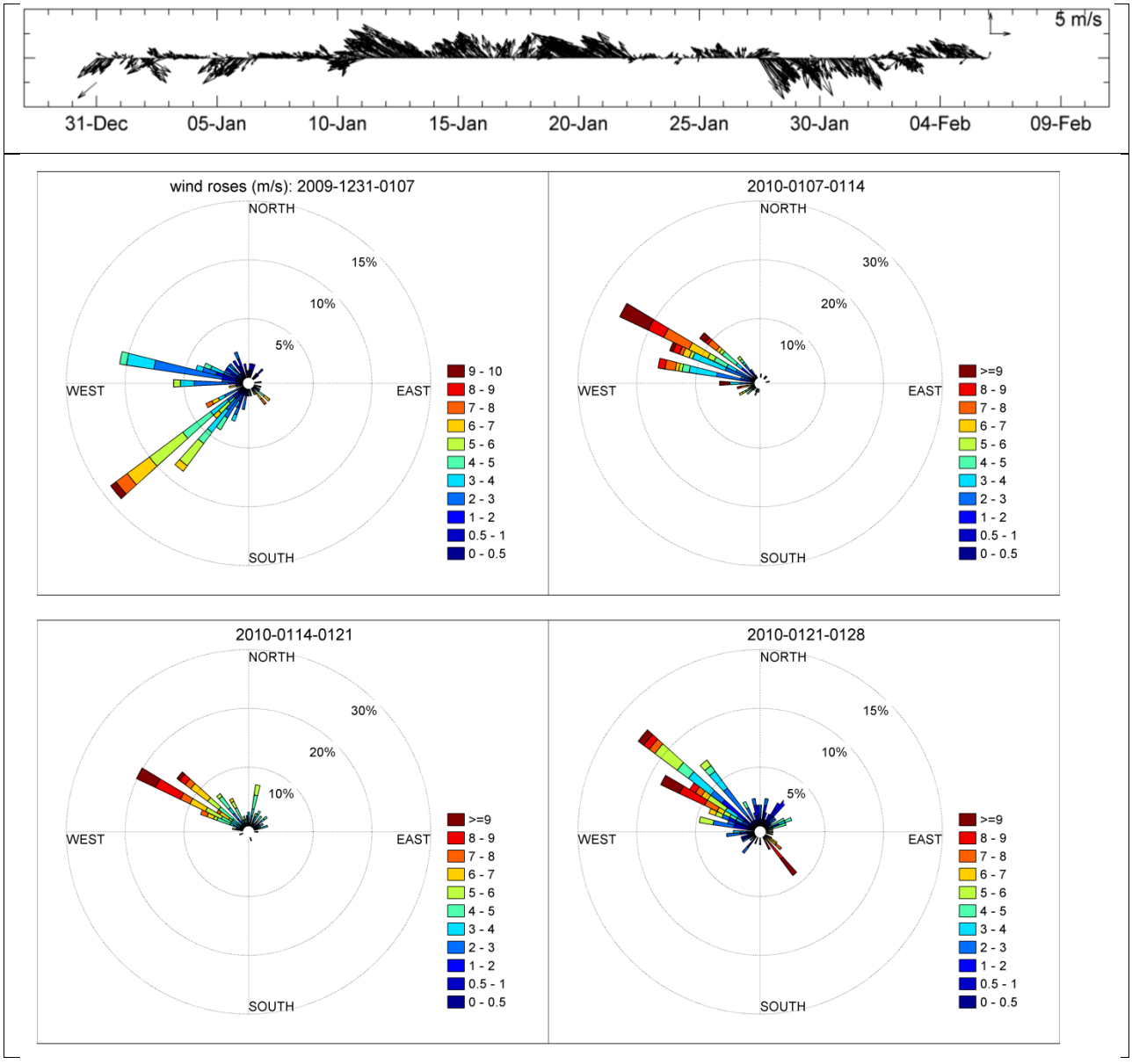

Figure 6 a. Wind vectors (3h average) and wind roses (from DWS) plotted separately for weeks 1-4 in January 2010 (**c**). The strongest East-South-Easterlies observed in a week-2, when the speed was over 9 m/s more than 25% of time.

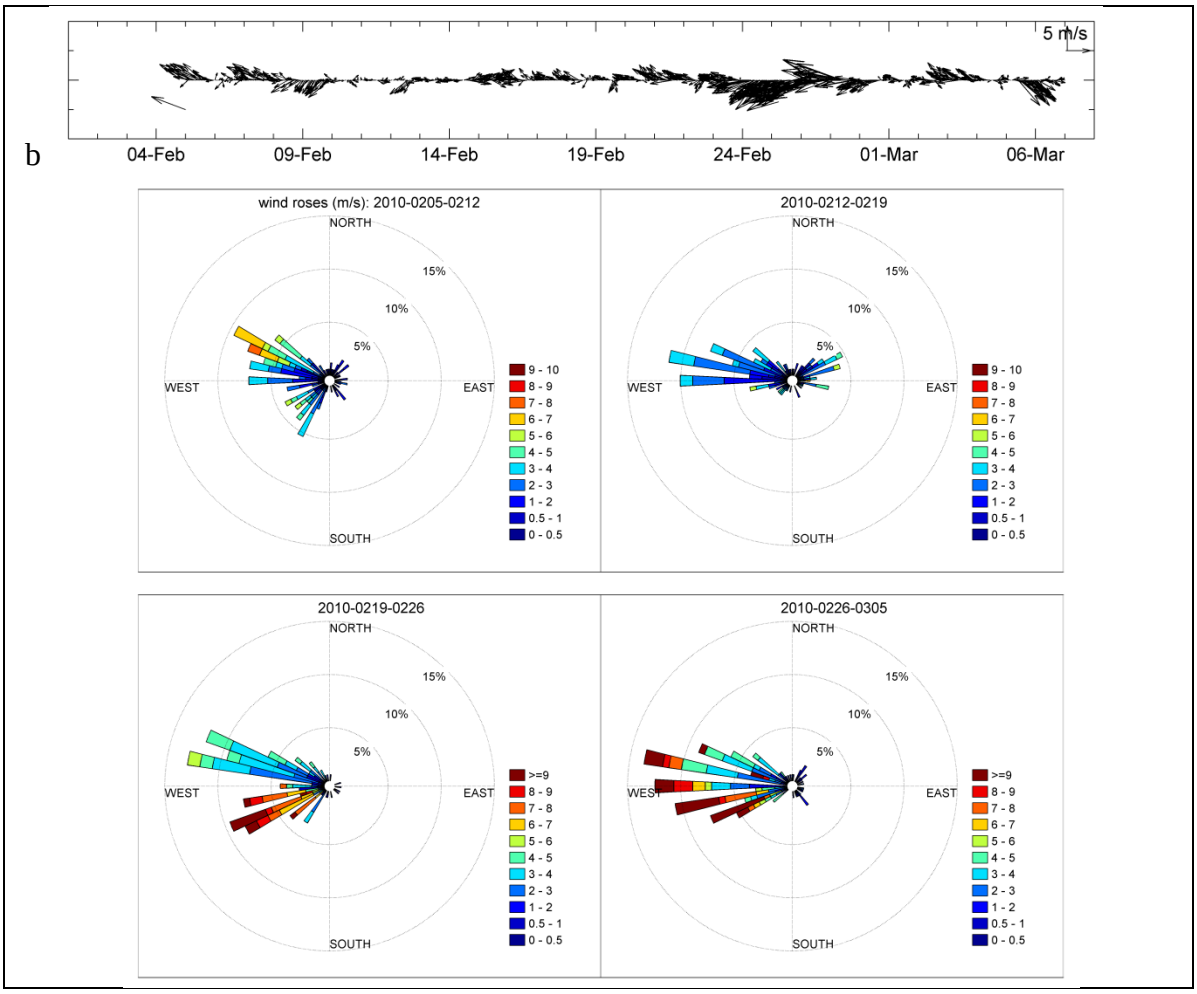

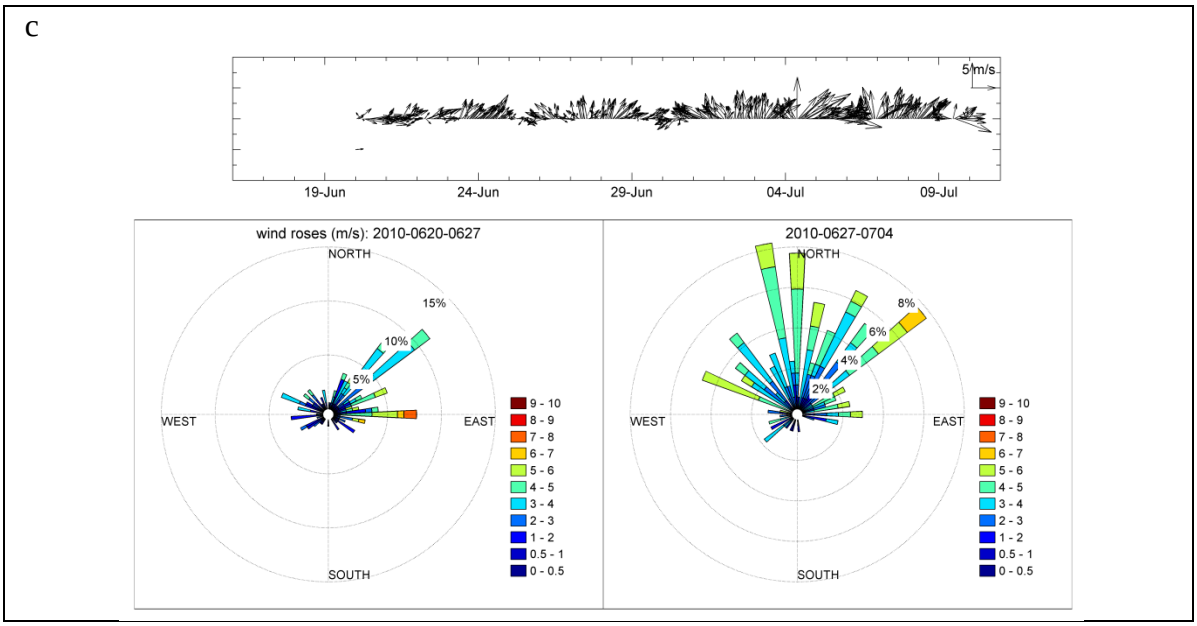

Figure 6 b,c. Wind roses (from DWS) plotted separately for each week in February 2010 (b) and June-July 2010(c). Note the scales are changed on each plot.

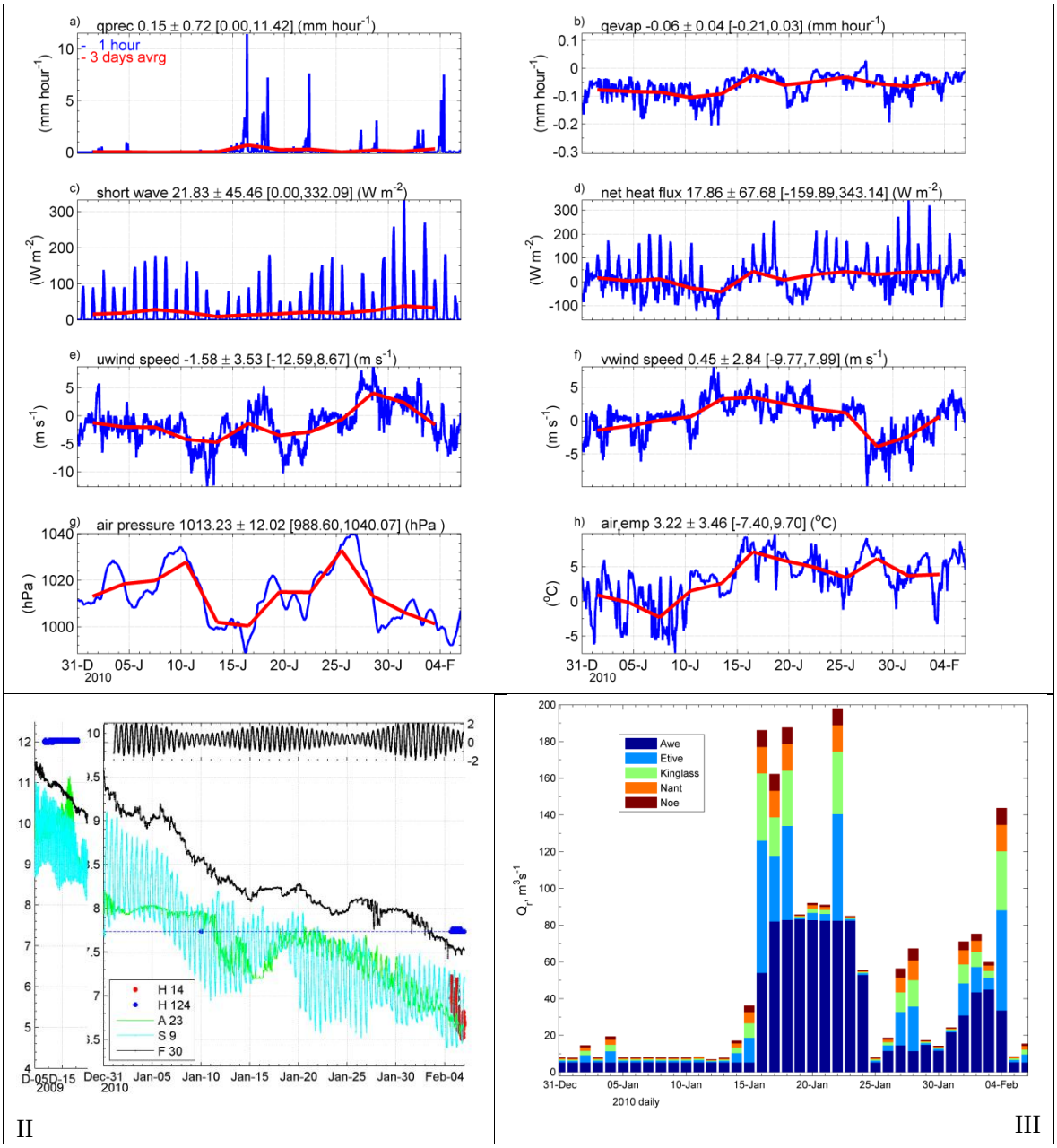

Figure 7. Meteorological parameters from Dunstaffnage Weather Station (Met-Office BADC ukmo-midas) hourly (blue) and 3-day running-average (red) during *the first overturning in January 2010* are shown at Panel **I**: a) precipitation, b) evaporation, c) short wave radiation, d) net heat flux, e) east-west and f) north-south wind components, g) air pressure at sea level and h) air temperature. The average, standard deviation and the range are shown above the graphs. Sea water temperature (ºC) for the same time from moorings at HYPOX site (124 m – blue; 14 m – red) in a deep basin, Airds bay (22m, green), next to the fjord entrance at Saulmore (9 m, light blue), and Foram (30 m, black) points, and tidal elevation (in Oban bay) are shown at Panel **II.** Note the change in T-scale between Dec 2009 and Jan 2010**.** Daily rivers discharge rates (m^3s^{-1}) are shown at Panel **III**.

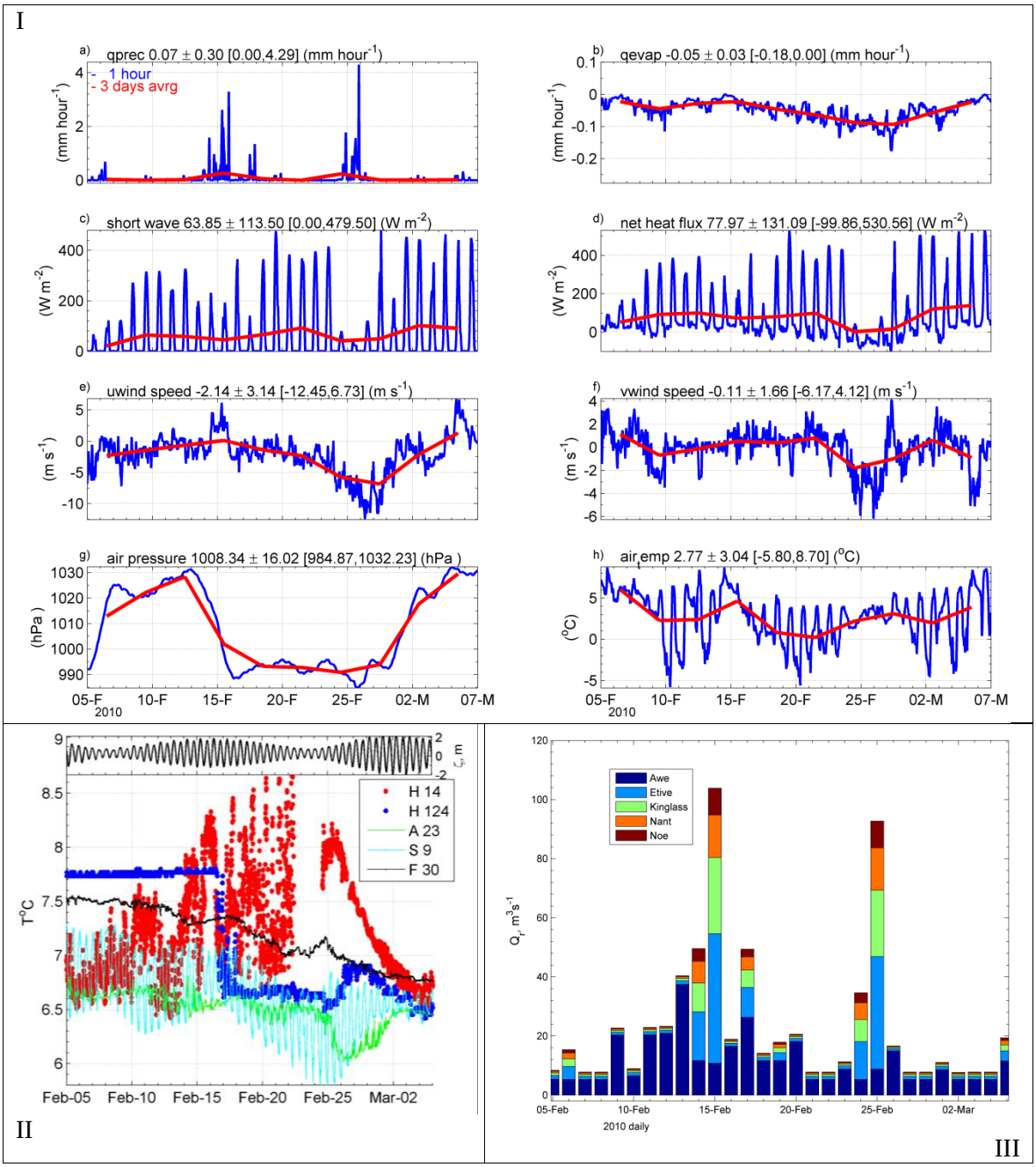

Figure 8. Meteo-parameters from DWS (I),Temperature Records from mooring (II) and daily river discharge (III) as on **Fig. 5**, during overturning event 2 (start on 16 Feb 2010, 23:00 GMT).

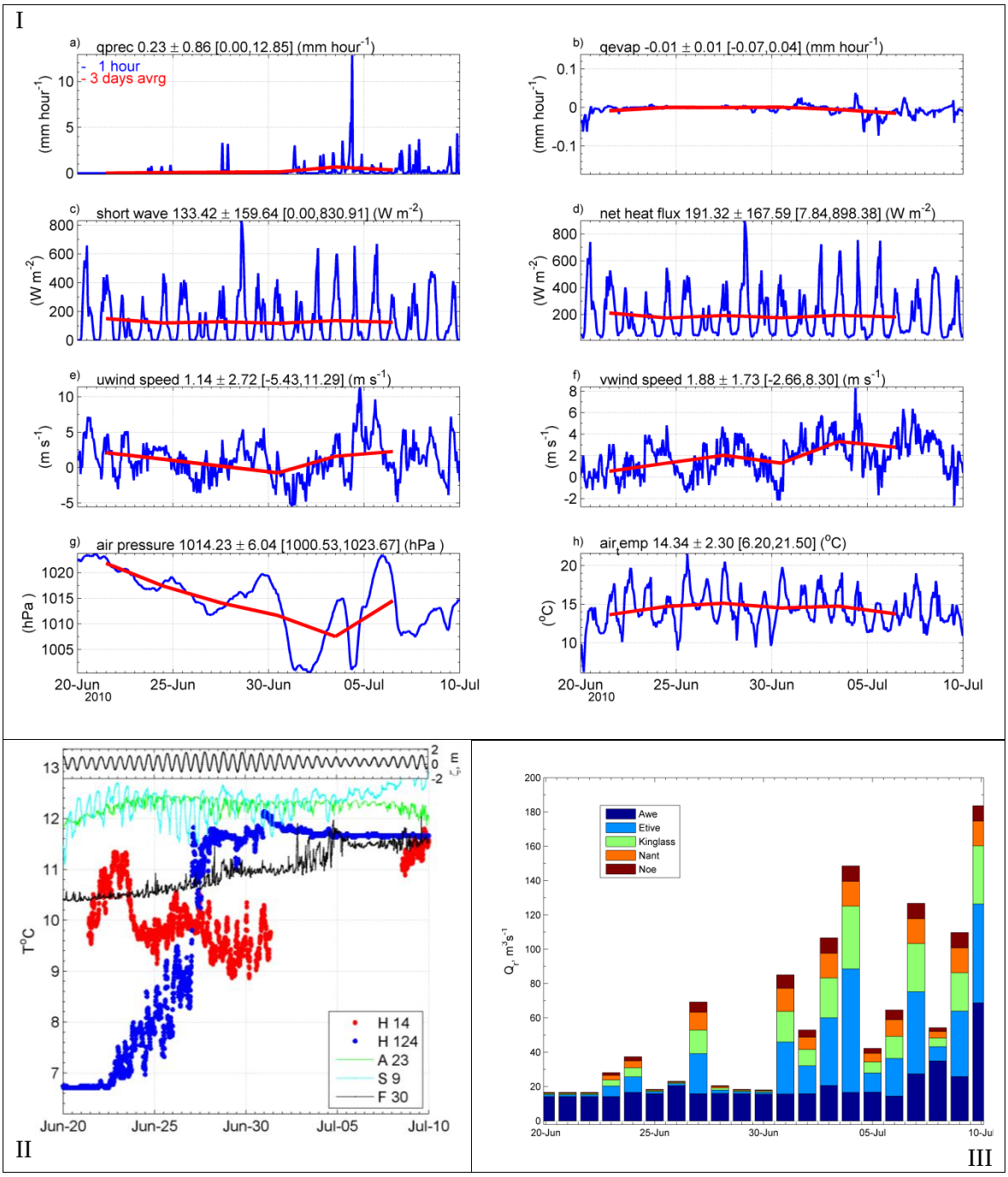

Figure 9. Meteo-parameters from DWS (I),Temperature Records from mooring (II) and daily river discharge (III) as on **Fig. 5** during *overturning event 3* (start on 22 June 2010, 20:00 GMT).

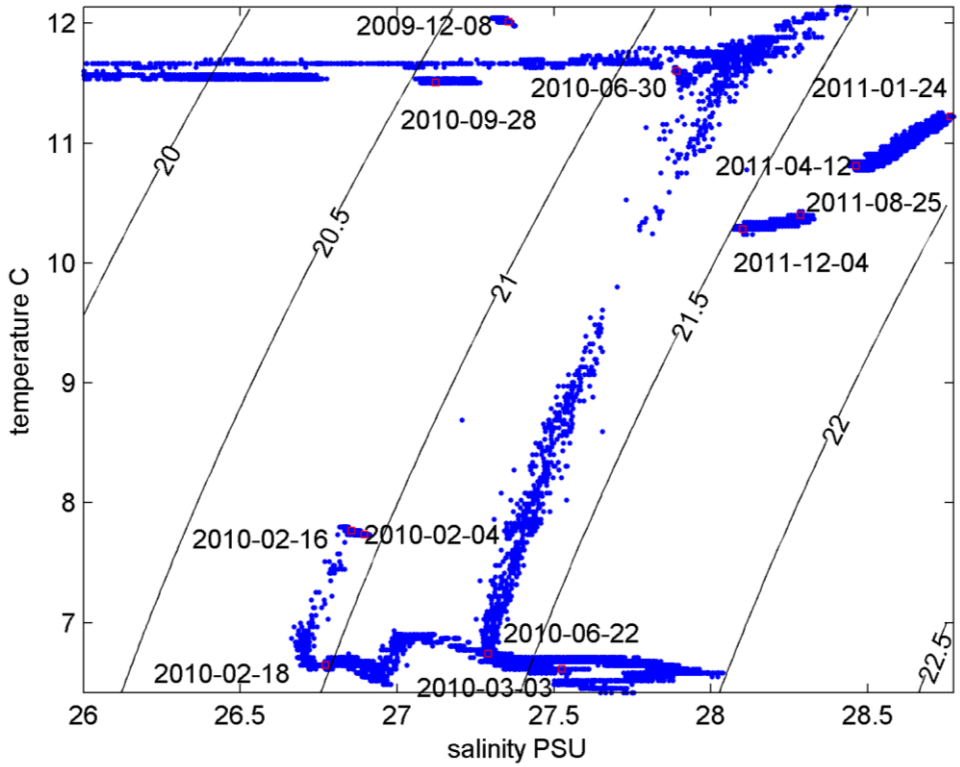

Figure 10 a. TS diagram shows the variations of sea water parameters from RDCP600 instrument deployed at Hypox mooring site at depth 124 m. Note the overturnings marks in 18 February – 3 March and 22– 30 June 2010.

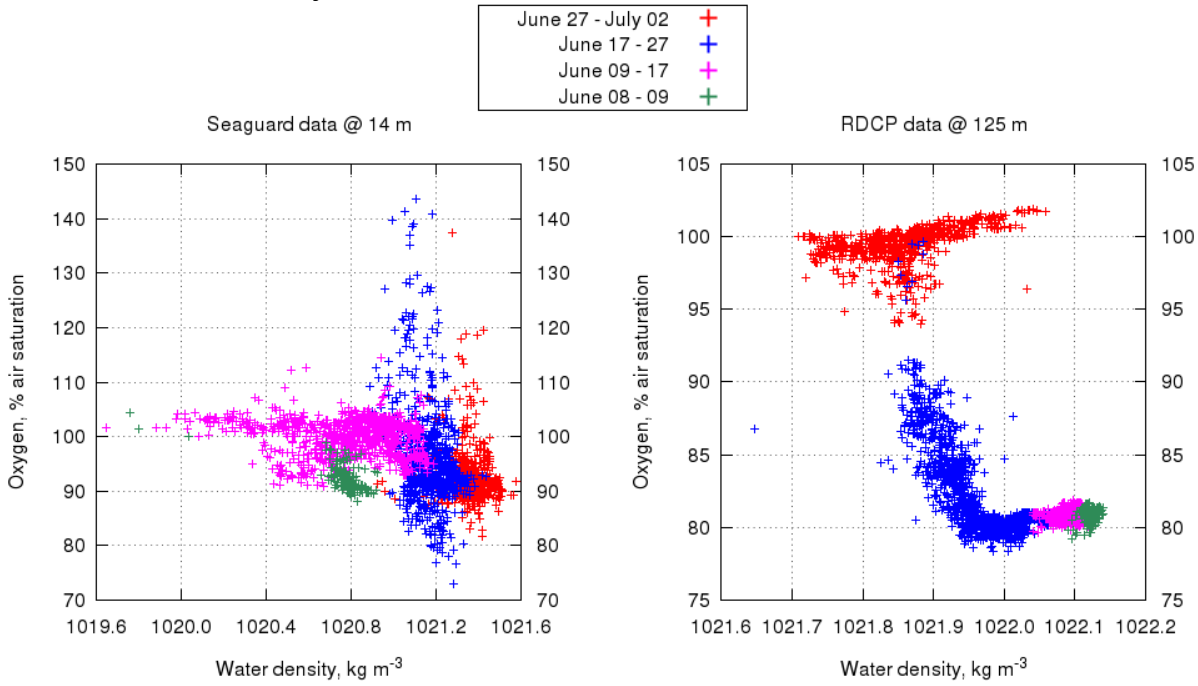

Figure 10 b,c. O_2-σ_Θ diagram shows the temporal evolution of dissolved oxygen (% of saturation) during the 3rd overturning in June 2010 (*Thanks to M. Kolonetz for the plot*).

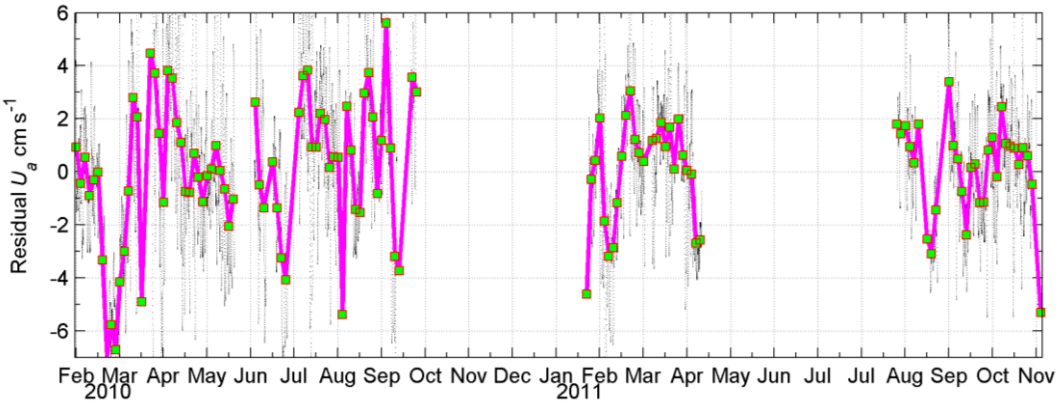

Figure 11. RCM-11 data from 14 m depth rotated along sea-loch axis (47.1°): residual velocity (black dots) measured every 15 minutes and 3-daily averaged residual velocity (squares).

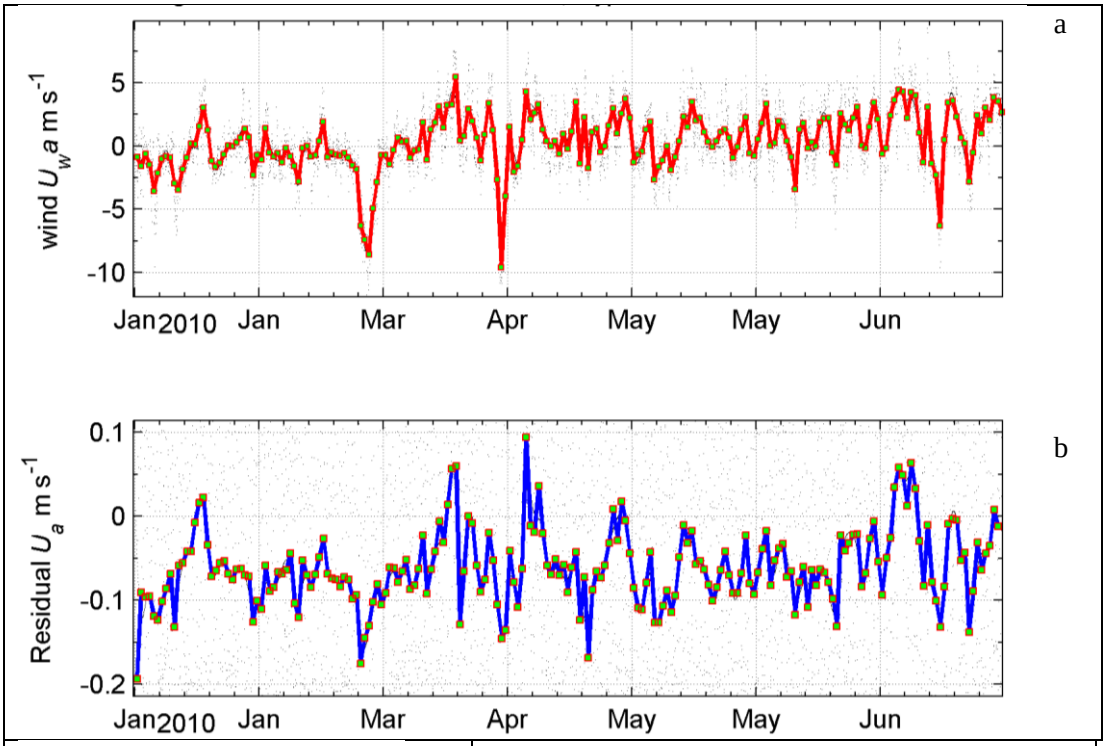

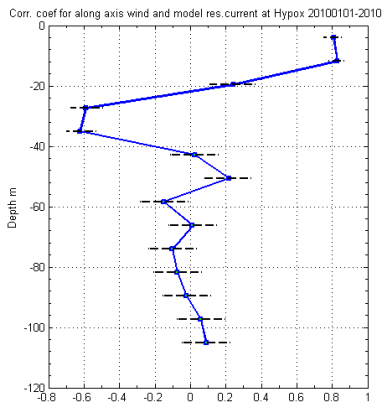

Figure 12. The amplitude of the winds at Dunstaffnage rotated clockwise with 47.1° along the loch Etive axis **(a)** measured (black dots) and daily-average (red). Residual along-axis velocity at sea surface form the model centroid nearest to the mooring site **(b)** hourly values (black dots), and daily-average (blue) from the run for January-July 2010. (**c**) Vertical distribution of these correlation coefficients, 95% CI shown with bars.

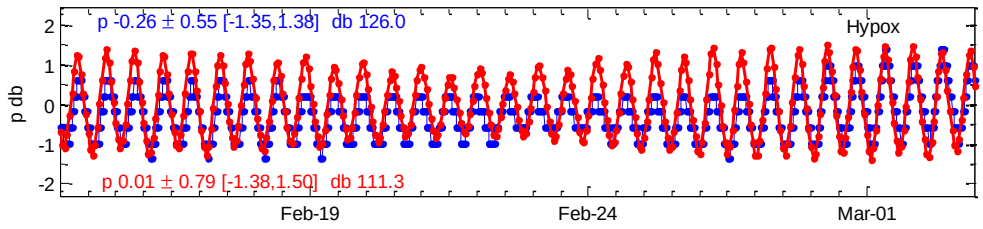
p -0.26 ± 0.55 [-1.35,1.38] db 126.0
Hypox
p 0.01 ± 0.79 [-1.38,1.50] db 111.3
p db
Feb-19
Feb-24
Mar-01

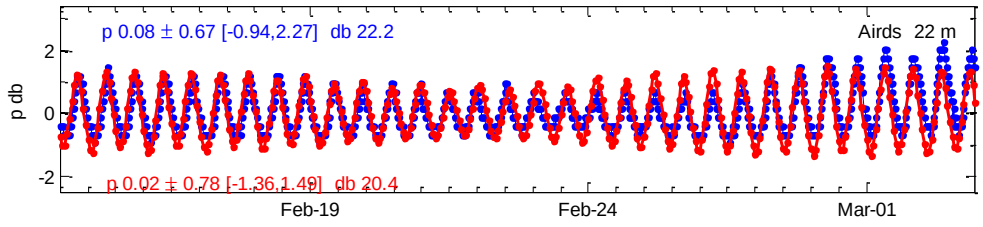
p 0.08 ± 0.67 [-0.94,2.27] db 22.2
Airds 22 m
p 0.02 ± 0.78 [-1.36,1.49] db 20.4
p db
Feb-19
Feb-24
Mar-01

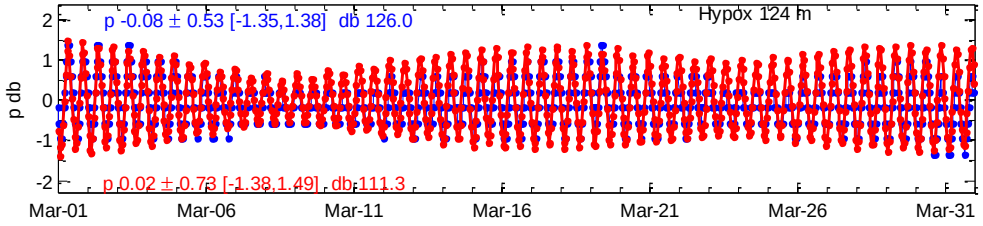
p -0.08 ± 0.53 [-1.35,1.38] db 126.0
Hypox 124 m
p 0.02 ± 0.73 [-1.38,1.49] db 111.3
p db
Mar-01
Mar-06
Mar-11
Mar-16
Mar-21
Mar-26
Mar-31

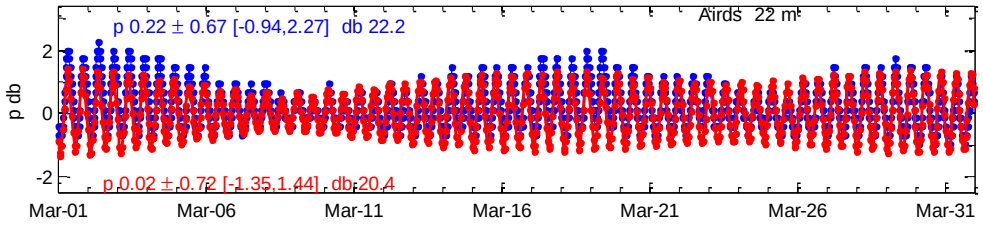
p 0.22 ± 0.67 [-0.94,2.27] db 22.2
Airds 22 m
p 0.02 ± 0.72 [-1.35,1.44] db 20.4
p db
Mar-01
Mar-06
Mar-11
Mar-16
Mar-21
Mar-26
Mar-31

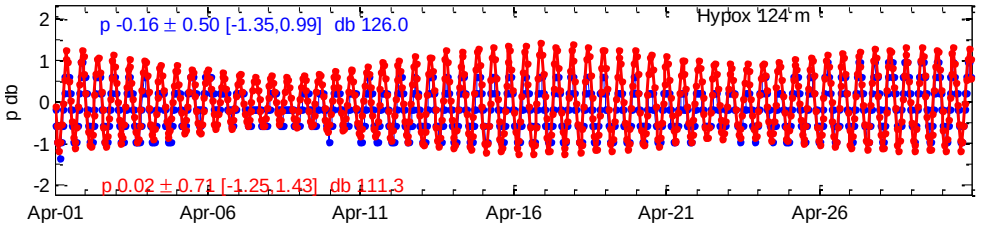
p -0.16 ± 0.50 [-1.35,0.99] db 126.0
Hypox 124 m
p 0.02 ± 0.71 [-1.25,1.43] db 111.3
p db
Apr-01
Apr-06
Apr-11
Apr-16
Apr-21
Apr-26

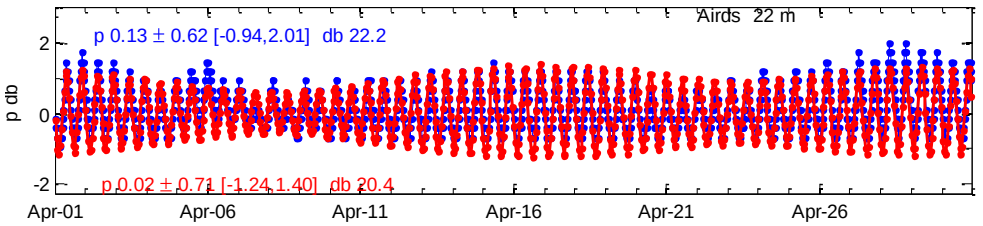
p 0.13 ± 0.62 [-0.94,2.01] db 22.2
Airds 22 m
p 0.02 ± 0.71 [-1.24,1.40] db 20.4
p db
Apr-01
Apr-06
Apr-11
Apr-16
Apr-21
Apr-26

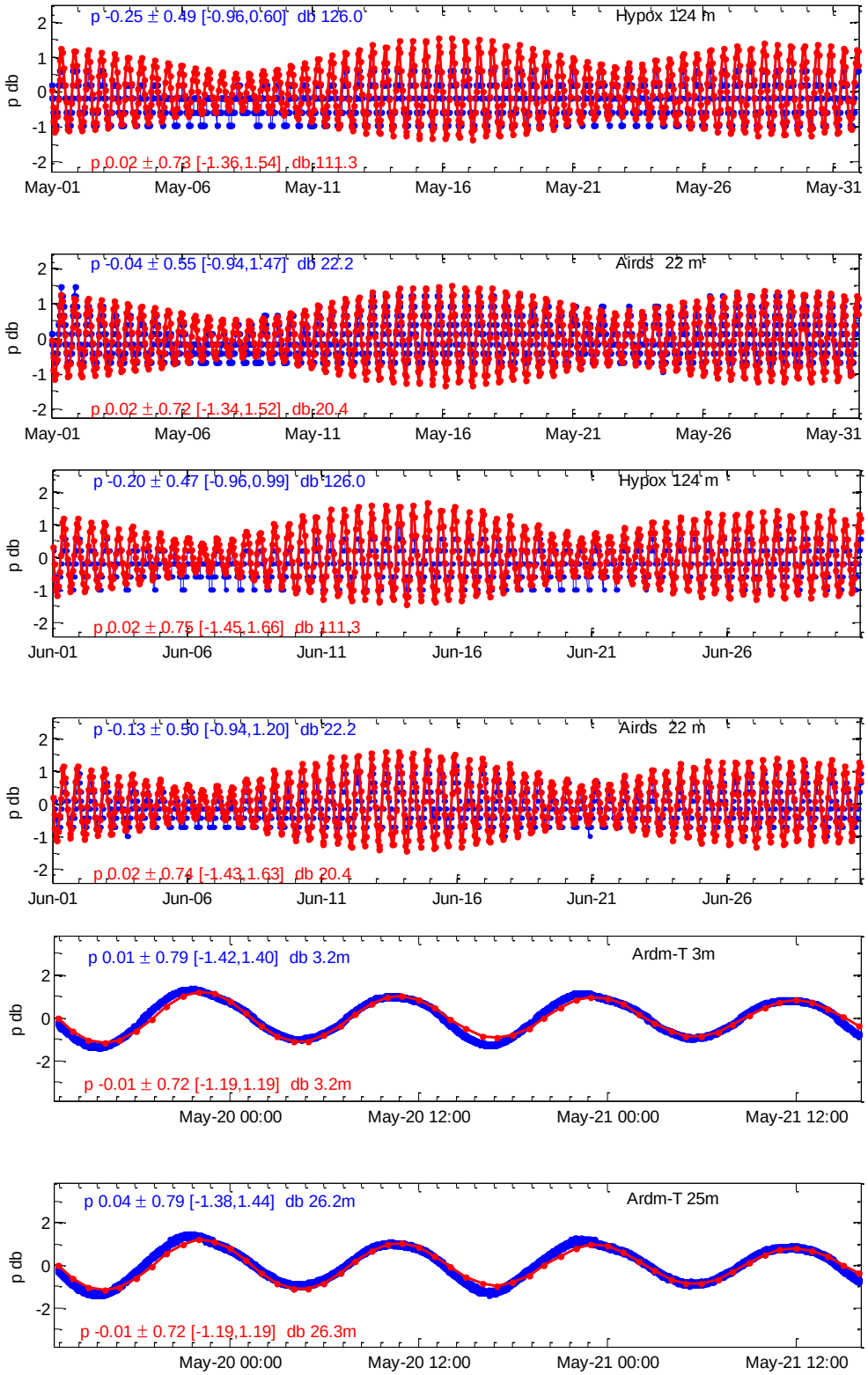

Figure 13. Model validation: normalised pressure time-series from the moorings (blue) and sea-surface elevation from the nearest node of the 15-layers model for Feb-April 2010 (red): (a-b) Hypox and Airds bay, (c-d) Ardmucknish bay (May).

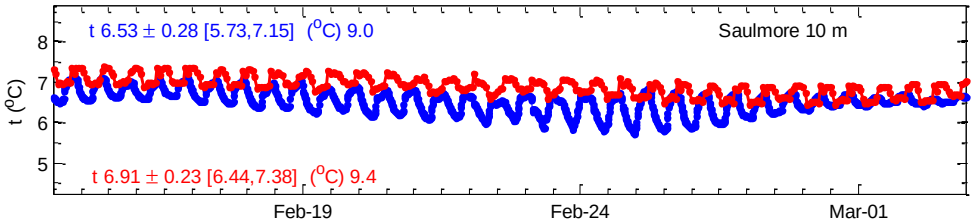
t 6.53 ± 0.28 [5.73,7.15] (°C) 9.0
Saulmore 10 m
t 6.91 ± 0.23 [6.44,7.38] (°C) 9.4
t (°C)
Feb-19
Feb-24
Mar-01

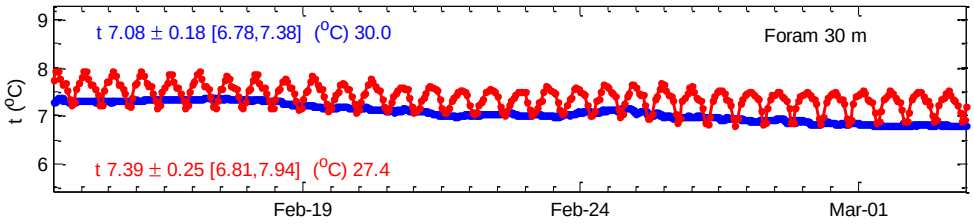
t 7.08 ± 0.18 [6.78,7.38] (°C) 30.0
Foram 30 m
t 7.39 ± 0.25 [6.81,7.94] (°C) 27.4
t (°C)
Feb-19
Feb-24
Mar-01

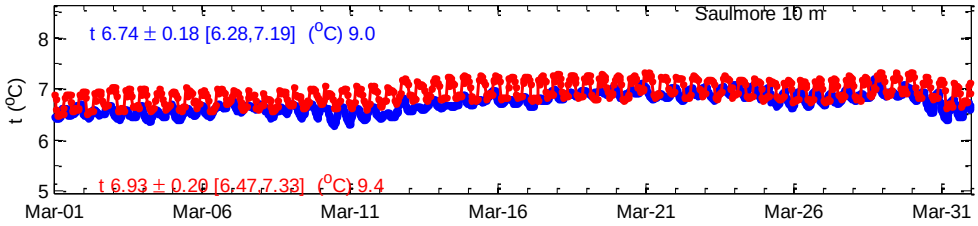
t 6.74 ± 0.18 [6.28,7.19] (°C) 9.0
Saulmore 10 m
t 6.93 ± 0.26 [6.47,7.33] (°C) 9.4
t (°C)
Mar-01
Mar-06
Mar-11
Mar-16
Mar-21
Mar-26
Mar-31

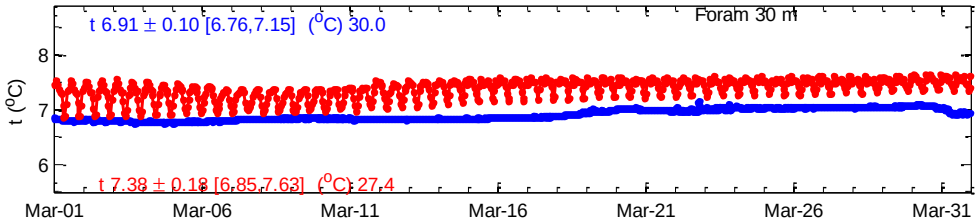
t 6.91 ± 0.10 [6.76,7.15] (°C) 30.0
Foram 30 m
t 7.38 ± 0.18 [6.85,7.63] (°C) 27.4
t (°C)
Mar-01
Mar-06
Mar-11
Mar-16
Mar-21
Mar-26
Mar-31

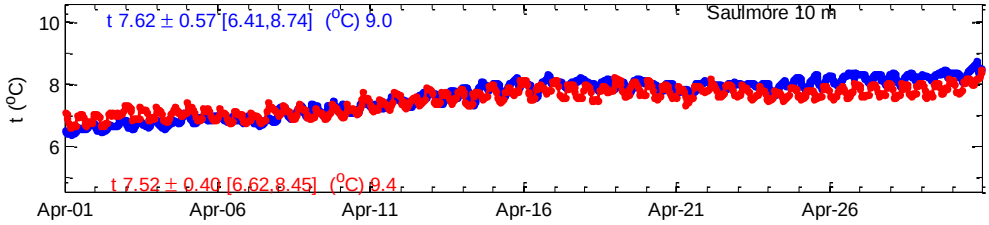
t 7.62 ± 0.57 [6.41,8.74] (°C) 9.0
Saulmore 10 m
t 7.52 ± 0.40 [6.62,8.45] (°C) 9.4
t (°C)
Apr-01
Apr-06
Apr-11
Apr-16
Apr-21
Apr-26

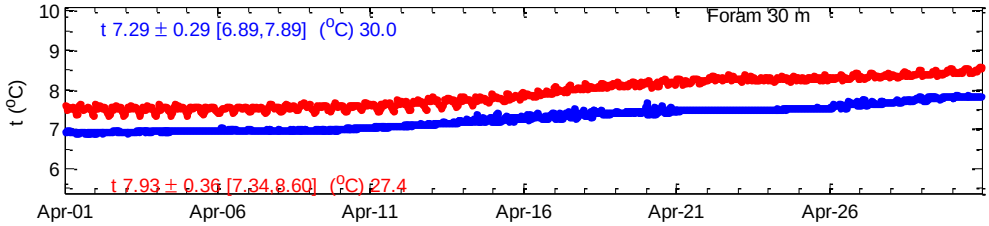
t 7.29 ± 0.29 [6.89,7.89] (°C) 30.0
Foram 30 m
t 7.93 ± 0.36 [7.34,8.60] (°C) 27.4
t (°C)
Apr-01
Apr-06
Apr-11
Apr-16
Apr-21
Apr-26

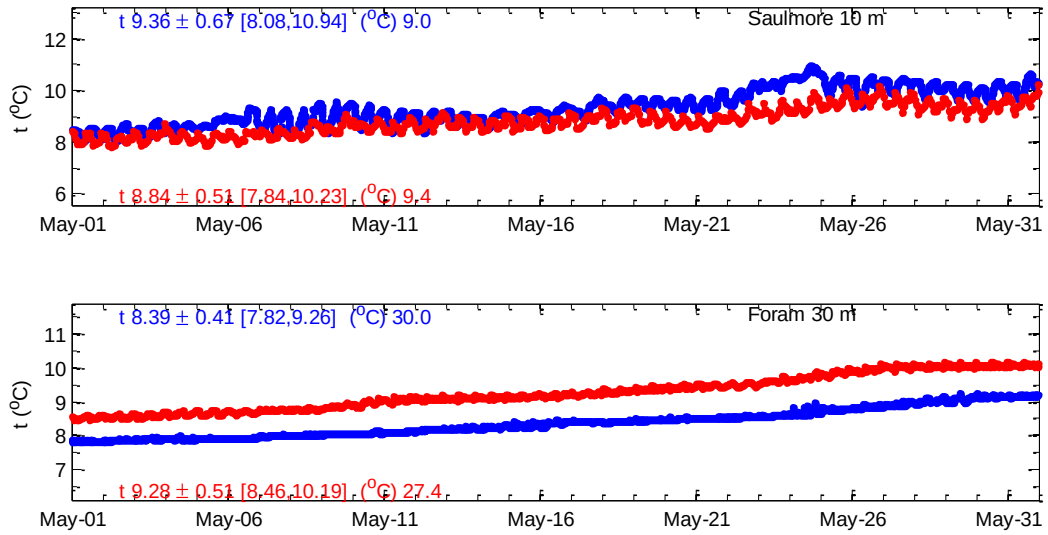

Figure 14. Model validation: temperature time-series from the mooring (blue) and from the nearest node of the 15-layer model (red) in Feb-May 2010: a) Saulmore, b) Foram points.

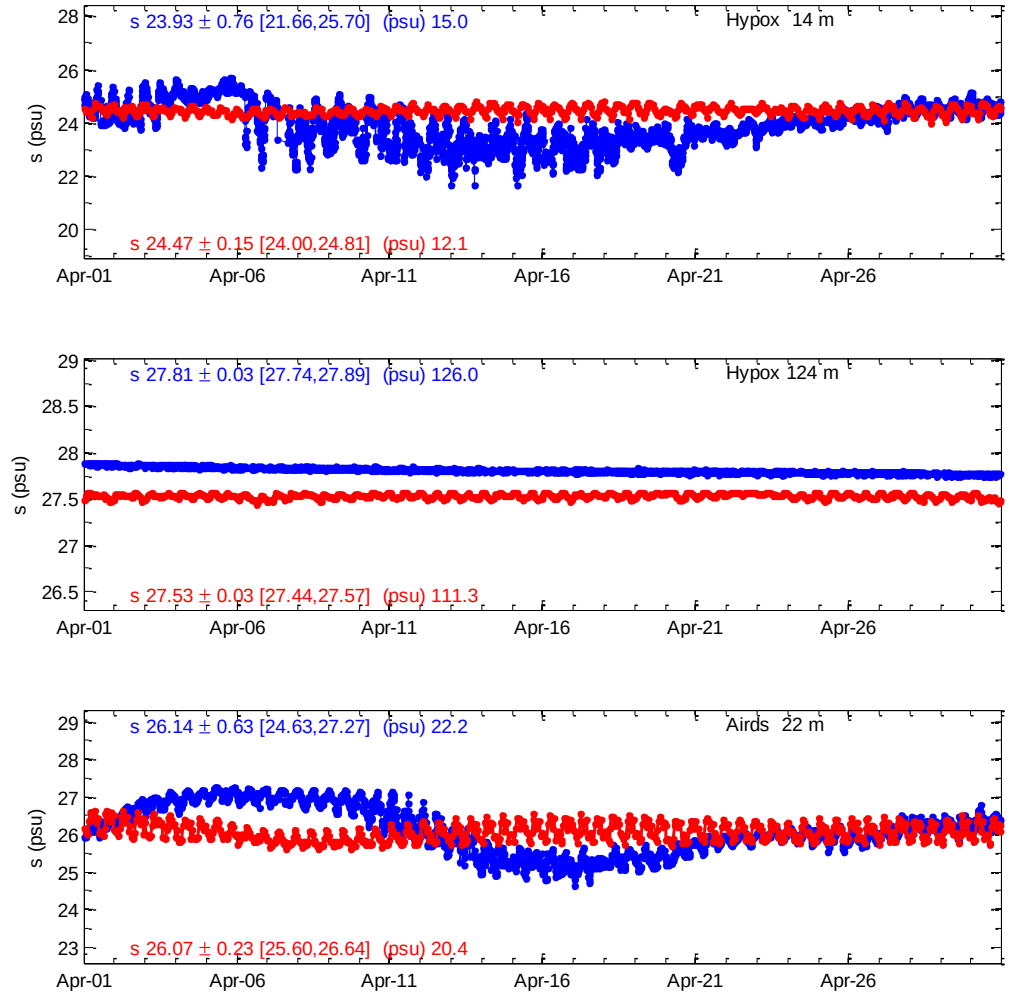

Figure 15. Model validation: salinity time-series from the mooring (blue) and from the nearest node of the 15-layers model (red) in April 2010: (a-b) Hypox 14 & 124 m, Airds Bay (c).

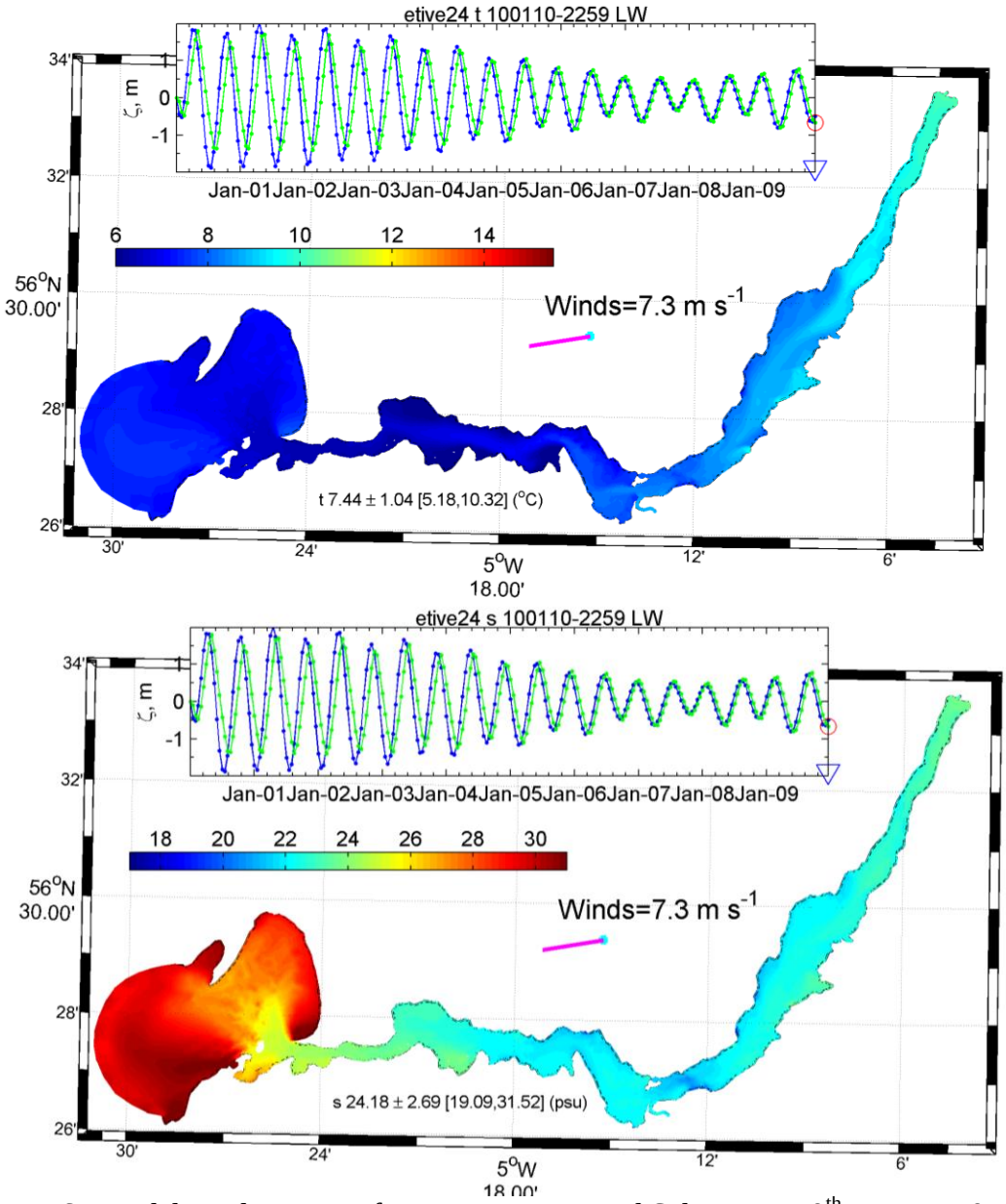

Figure 16. Model results: sea surface Temperature and Salinity on 10th January 2010.

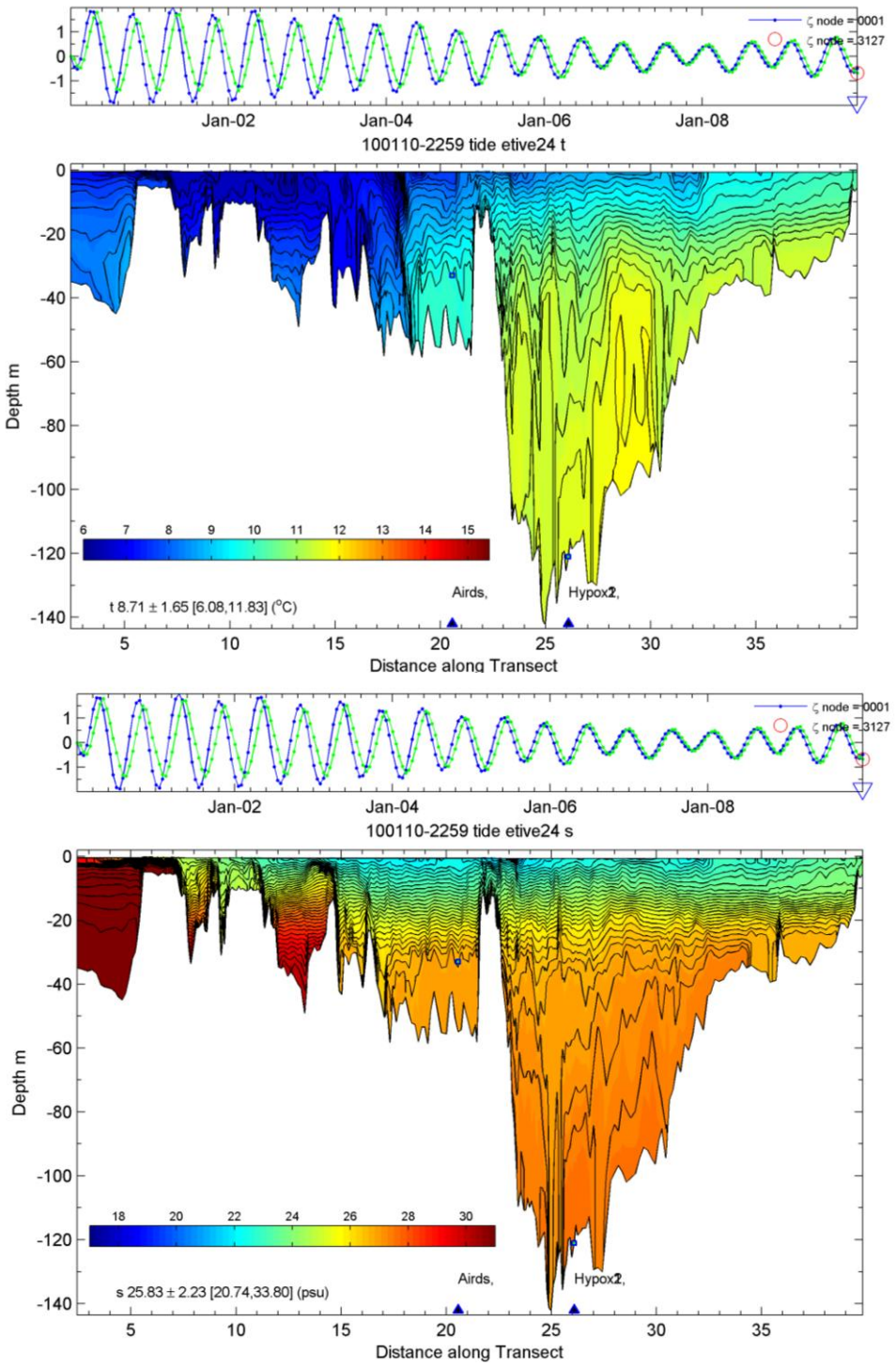

Figure 17. Model results: vertical transects of Temperature and Salinity for 10th January 2010.

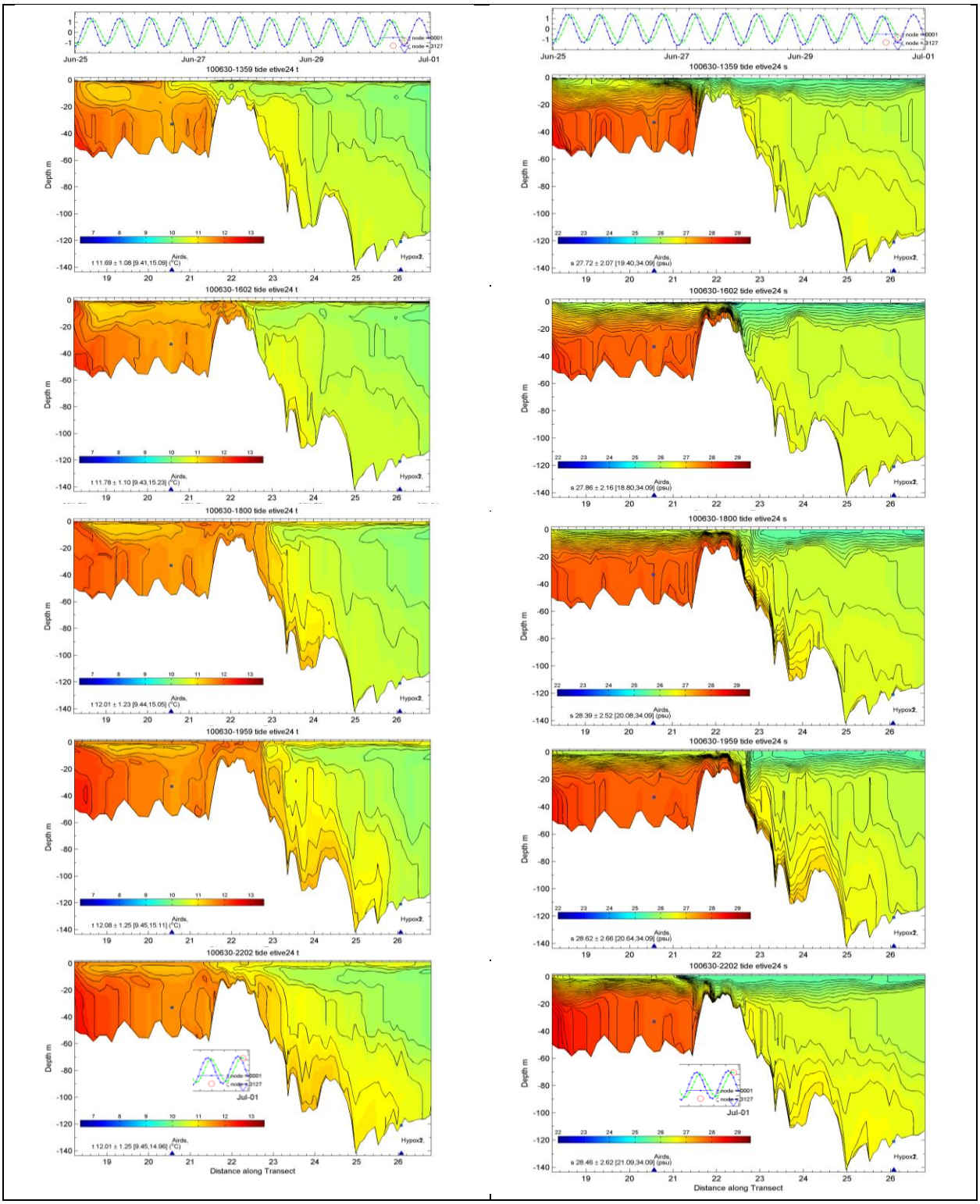

Figure 18. Model results for simulation of June 2010 overturning event: transects of Temperature (left) and Salinity (right) during a single flood-ebb cycle.

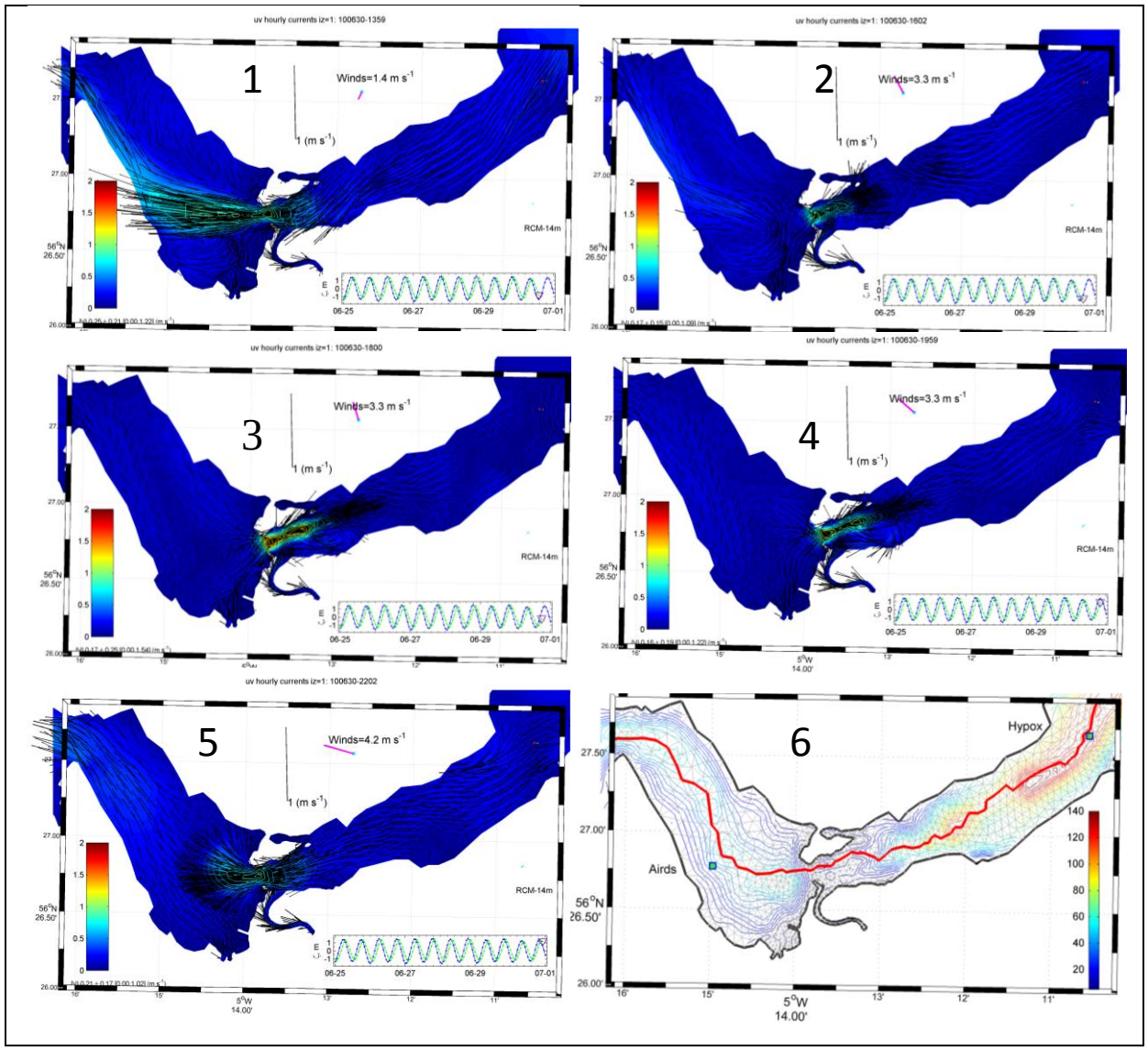

Figure 19. Model results for simulation of June 2010 overturning event: sea surface velocity during a single flood-ebb cycle (1-5) with two hours interval, the colour-scale corresponds to velocity magnitude ($m \cdot s^{-1}$). The bathymetry (m) and the along-axis transect line (**Fig.18**), are also shown (6).

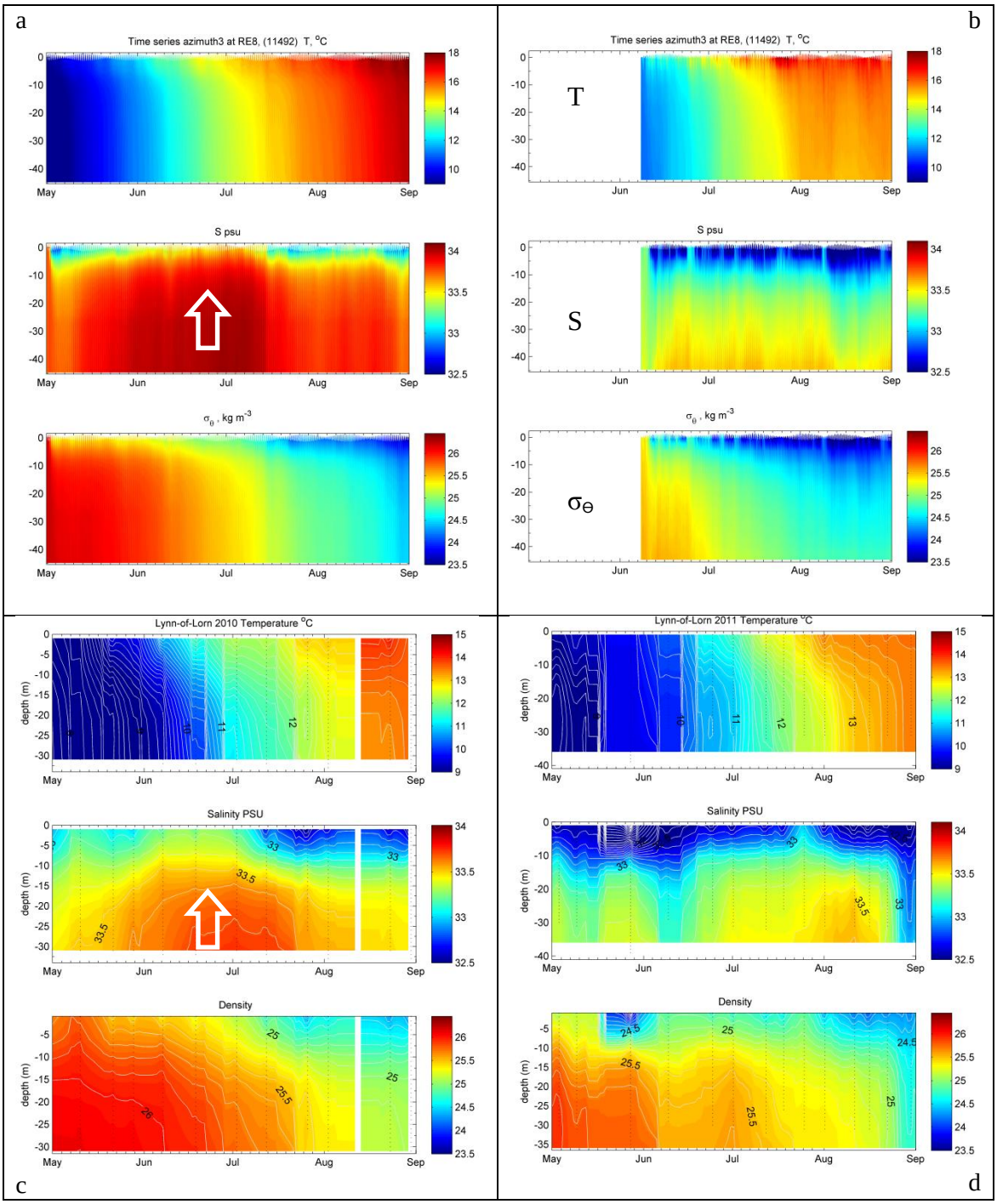

Figure 20. Time series (Temperature, Salinity and Potential Density) near the open boundary of the Loch Etive FVCOM Model in Ardmucknish Bay in summer 2010 (a) and 2011 (b) from the Firth of Lorn FVCOM Model. Weekly time-series form the nearest (LY1) station in the Lynn-of-Lorne (56º 28.91'N, 5º 30.10'W) in summer 2010(c) and 2011(d).

Tables

Table 1. Loch Etive geometry and hydrography [Edwards,Sharples, 1991]

Loch length	29.5	km
Tidal range	1.8	m
Max. Depth	145	m
Mean Depth	33.9	m
High W. Area	29.5	km^2
Low W. Area	27.7	km^2
Low W. Volume	$939.8 \cdot 10^6$	m^3
Watershed	1350	km^2
Rainfall annual	2500	mm
Runoff annual	$3037.5 \cdot 10^6$	m^3

Table 2. Loch Etive sills geometry adapted from (Edwards, Sharples, 1991)

Sill N°/ Name	Length	High Water Width	Low Water Width	Max Depth	Mean Depth	Cross-Section Area	Shape Length
	m	m	m	m	m	m²	m
1	1990	440	420	9	7	2900	682.2
2 Connel	320	240	220	7	4	850	223.1
3	1380	460	440	8	5	2000	428.9
4	240	720	700	12	8	5600	675.4
5	540	750	730	24	12	8900	709.7
6 BonAwe	680	220	200	13	8	1500	238.7

Table 3. Vertical diffusion coefficients ($m^2 \cdot s^{-1}$) in a deep layer from CTD casts at the Hypox mooring site during stagnation period.

	26 Aug 2010	13 January 2012	
Depth, m	50-115	70-115	↓
K_{zT}	$8.2 \cdot 10^{-3}$	$4.6 \cdot 10^{-2}$	↑
K_{zS}	$1.0 \cdot 10^{-2}$	$1.5 \cdot 10^{-4}$	↓
K_{zO_2}	$2.4 \cdot 10^{-2}$	$5.1 \cdot 10^{-4}$	↓

Table 4. Tidal constituents for Oban (56º24'N, 5 º 28'W) based on long term observations, International Hydrographic Office.

	M2	**N2**	**S2**	**K2**	**O1**	**K1**
Amplitude, m	1.069	0.203	0.458	0.148	0.069	0.069
Phase, º	154.9	146	201	198	35	182

Table 5. Statistical valuations of the model performance for 7-month sea level time series.

Site	Observations		Model		Correlation coefficient	RMSE	Index of agreement
	Mean m	Std. Dev. m	Mean m	Std. Dev. m		m	d
Hypox	-0.18	0.49	0.02	0.73	0.89	0.42	0.88
Airds	0.03	0.60	0.02	0.73	0.84	0.39	0.91
Mean					0.86	0.41	0.89

Table 6. Statistical valuations of the model performance for 7-month temperature time series.

Site	Observations		Model		Correlation coefficient	RMSE	Index of agreement
	Mean ºC	Std. Dev. ºC	Mean ºC	Std. Dev. ºC		ºC	d
Saulmore	8.90	2.30	8.36	1.56	0.98	1.01	0.93
Foram	8.57	1.65	9.13	1.81	0.98	0.69	0.96
mean					0.98	0.85	0.94